A Tsunami Forecast Model for Ponce, Puerto Rico

Dylan Righi

Contents

Abstract

In support of the National Oceanic and Atmospheric Administration's tsunami forecast system, we have developed and tested a numerical tsunami model for the community of Ponce, Puerto Rico. The Ponce tsunami forecast model employs the optimized version of the Method of Splitting Tsunami (MOST) numerical code and has been validated and tested using data from a set of 8 synthetically generated tsunami events (6 mega-events forced by Mw 9.3 earthquakes, a medium Mw 7.5, and a micro-event) from around the Atlantic Ocean basin. A high-resolution reference model, without limitations on computational run-times, has also been developed to provide comparison for the forecast model. Validation results show good agreement between the forecast and reference models. The forecast model is shown to be stable under forcing from both large and small modeled tsunami events and will provide dependable warnings in the event of a tsunami that might threaten the people and resources of Ponce.

1.0 Background and Objectives

The National Oceanic and Atmospheric Administration (NOAA) Center for Tsunami Research (NCTR) at the NOAA Pacific Marine Environmental Laboratory (PMEL) has developed a tsunami forecasting capability for operational use by NOAA's two Tsunami Warning Centers located in Hawaii and Alaska (Titov *et al.*, 2005). The system is designed to efficiently provide basin-wide warning of approaching tsunami waves accurately and quickly. The system, termed Short-term Inundation Forecast of Tsunamis (SIFT), combines real-time tsunami event data with numerical models to produce estimates of tsunami wave arrival times and amplitudes at a coastal community of interest. The SIFT system integrates several key components: deep-ocean observations of tsunamis in real time, a basin-wide pre-computed propagation database of water level and flow velocities based on potential seismic unit sources, an inversion algorithm to refine the tsunami source based on deep-ocean observations during an event, and high-resolution tsunami forecast models.

Ponce, Puerto Rico is the islands second largest city in terms of population and area. It sits on the central southern coast of Puerto Rico. Its population, as reported by the 2010 US census,

was 166,327 (a 10% decrease from the 2000 census). The economic base of the city is quite varied – with tourism, manufacturing, retail and government being the main employers. Shipping, through the Port of Ponce, is also a source of jobs in the region and there are plans to develop a mega-port that will increase the number of cargo and cruise ships docking in Ponce. A map of Ponce is shown in Figure 1.

The goal of this work is to provide a high quality forecast model that will enable tsunami forecasters to quickly and correctly advise emergency planners at the local, state and national levels in their efforts to protect the people and resources of Ponce and surrounding areas from the dangers of tsunami events.

2.0 Forecast Methodology

A high-resolution inundation model was used as the basis for development of a tsunami forecast model to operationally provide an estimate of wave arrival time, wave height, and inundation at Florence following tsunami generation. All tsunami forecast models are run in real time while a tsunami is propagating across the open ocean. The Ponce model was designed and tested to perform under stringent time constraints given that time is generally the single limiting factor in saving lives and property. The goal of this work is to maximize the length of time that residents of the area have to react to a tsunami threat by providing accurate information quickly to emergency managers and other officials responsible for the community and infrastructure.

The general tsunami forecast model, based on the Method of Splitting Tsunami (MOST), is used in the tsunami inundation and forecasting system to provide real-time tsunami forecasts at selected coastal communities. The model run-times are on the order of a few minutes, and employ high-resolution grids constructed by the National Geophysical Data Center. The Method of Splitting Tsunami (MOST) is a suite of numerical simulation codes capable of simulating three processes of tsunami evolution: earthquake, transoceanic propagation, and inundation of dry land. The MOST model has been extensively tested against a number of laboratory experiments and benchmarks (Synolakis *et al.*, 2008) and was successfully used for simulations of many historical tsunami events. The main objective of a forecast model is to

provide an accurate, yet rapid, estimate of wave arrival time, wave height, and inundation in the minutes following a tsunami event. Titov and González (1997) describe the technical aspects of forecast model development, stability, testing, and robustness, and Tang *et al.,* 2009 provide detailed forecast methodology.

A basin-wide database of pre-computed water elevations and flow velocities for unit sources covering worldwide subduction zones has been generated to expedite forecasts (Gica *et al.,* 2008). As the tsunami wave propagates across the ocean and successively reaches tsunameter observation sites, recorded sea level is ingested into the tsunami forecast application (SIFT) in near real-time and input into an inversion algorithm that produces an improved estimate of the tsunami source. A linear combination of the pre-computed database is then performed based on this tsunami source, now reflecting the transfer of energy to the fluid body, to produce synthetic boundary conditions of water elevation and flow velocities to initiate the forecast model computation.

Accurate forecasting of the tsunami impact on a coastal community largely relies on the accuracies of bathymetry and topography and the numerical computation. The high spatial and temporal grid resolution necessary for modeling accuracy poses a challenge in the run-time requirement for real-time forecasts. Each forecast model consists of three nested grids with increasing spatial resolution in the finest grid, and temporal resolution for simulation of wave inundation onto dry land. The forecast model utilizes the most recent bathymetry and topography available to reproduce the correct wave dynamics during the inundation computation. Forecast models, including the Ponce model, are constructed for at-risk populous coastal communities in the Pacific and Atlantic Oceans. Previous and present development of forecast models in the Pacific (Titov *et al.*, 2005; Titov, 2009; Tang *et al.*, 2008; Wei *et al.*, 2008) have validated the accuracy and efficiency of each forecast model currently implemented in the real-time tsunami forecast system. Models are tested when the opportunity arises during real events and are also used for scientific research. Tang *et al.*, 2009 provide forecast methodology details.

3.0 Model Development

The general methodology for modeling at-risk coastal communities is to develop a set of three nested grids, referred to as A, B, and C-grids, each of which becomes successively finer in resolution as they telescope into the population and economic center of the community of interest. The offshore area is covered by the largest and lowest resolution A-grid while the near-shore details are resolved within the finest scale C-grid to the point that tide gauge observations (if available) recorded during historical tsunamis are resolved within expected accuracy limits. The procedure is to begin development with large spatial extent merged bathymetric topographic grids at high resolution, and then optimize these grids by sub-sampling to coarsen the resolution and shrink the overall grid dimensions to achieve a 4 to 10 hour simulation of modeled tsunami waves within the required time period of 10 minutes of wall-clock time. The basis for these grids is a high-resolution digital elevation model constructed by the National Geophysical Data Center (NGDC) and NCTR using all available bathymetric, topographic, and shoreline data to reproduce the wave dynamics during the inundation computation for an at-risk community. For each community, data are compiled from a variety of sources to produce a digital elevation model referenced to Mean High Water in the vertical and to the World Geodetic System 1984 in the horizontal (http://ngdc.noaa.gov/mgg/inundation/tsunami/inundation.html). From these digital elevation models, a set of three high-resolution, "reference" elevation grids are constructed for development of a high-resolution reference model from which an 'optimized' model is constructed to run in an operationally specified period of time. The operationally developed model is referred to as the optimized tsunami forecast model or forecast model for brevity.

Development of an optimized tsunami forecast model for Ponce began with the merged bathymetric/topographic grid covering all of Puerto Rico provided by the National Geophysical Data Center (Taylor et.al., 2007) shown in Figure 2. The author considers this to be an adequate representation of the local topography/bathymetry. As new digital elevation models become available, forecast models will be updated and report updates will be posted at http://nctr.pmel.noaa.gov/forecast_reports/. Grid dimension extension and additional information are updated as needed and appropriate. Grids are designed such that a significant portion of the modeled tsunami waves, typically 4 to 10 hr of modeled tsunami time, pass

through the model domain without appreciable signal degradation. Table 1 provides specific details of both reference and tsunami forecast model grids, including extents. Complete input parameter information for the model runs is provided in Appendix A.

3.1 Forecast Area

Ponce and its port are shown in the aerial image in Figure 3. The view, to the west, shows the town center in the upper center, and the small boat harbor and shipping docks in the foreground. Most of the city's residential and industrial areas are away from the coast behind coastal lowland marshes. As seen in the map in Figure 1, Highways 1 and 2 define the limit between town and marshes. The exceptions to this are the neighborhoods of Amalia Marin and Playa, the Port of Ponce industrial area, and the Ponce Yacht club and small boat harbor. The town center is located further inland. Mountains to the north border the town and most of neighborhoods are in the foothills.

The Ponce bay is fairly shallow, but depths begin to increase quickly less than 10 kilometers offshore. Further offshore to the south, the depths of the Caribbean Sea are greater than 4500 meters. North of the island, the deep Puerto Rico Trench is the dominant feature. This marks the complicated subduction zone between the North American and Caribbean plates and is a tectonically active region. The earthquake of 1918, discussed in the next section, originated on a fault associated with this subduction zone. Geological studies suggest that this subduction zone has not had a major rupture in over 200 years and could cause a major earthquake in the future. It's proximity to Ponce highlights the importance of developing high quality tsunami warning models and tools for the region.

3.2 Historical Events and Data

There is no dedicated tide gauge available at Ponce, Puerto Rico. The nearest tide gauges are located in Penuelas and Parguera (on Magueyes Island), 13 and 43 kilometers to the west, respectively. The Penuelas gauge is operated by the Puerto Rico Seismic Network and located at 17.973000 °N, 66.762000 °W. The Parguera gauge is located at 17.971667 °N, 67.046667 °W and is operated by the NOAA National Ocean Service. These points are not close enough to provide quality comparisons with our forecast model predictions. However, there are

historical accounts of tsunami run-up heights available from the National Geophysical and Data Center tsunami run-up database (http://www.ngdc.noaa.gov/nndc/struts/form?t=101650&s=167&d=166). A warning point consistent with these available data has been chosen for the Ponce models. The point is located on the eastern side of the Ponce bay, near the small boat harbor and docks. The absolute location of this point 17.9660 °N, N 66.6210 °W, and the forecast model grid depth at this location is 10.1 meters. For reference, this point is shown in Figure 1.

3.3 Model Setup

Accurate bathymetry and topography are crucial inputs to developing the reference and forecast models, especially for the inundation of the near-shore environment. To develop each grid, we attempt to gather and use the best available data for the area studied. Grids may be updated if newer, more accurate data become available. The grids developed for the Ponce reference and forecast models were derived from three main source grids - a Gulf Coast/Caribbean 9 arc-second resolution grid, a 1 arc-second Puerto Rico digital elevation model (DEM), and the 1/3 arc-second Ponce DEM (Taylor *et al*, 2007). All three grids were developed at the National Geophysical Data Center (NGDC). The 1/3 arc-second DEM was developed to cover the entire area surrounding Ponce and as such, covers the extent 67.1 to 66.4 °W, and 17.7 to 18.05 °N. At Ponce's latitude, 1/3 arc-second of longitude and latitude are equal to 9.8 and 10.2 meters, respectively. A topographic map of the source DEM is shown in Figure 4.

The grid extents and parameters of the developed forecast and reference model grids are detailed in Table 1. The lowest resolution A-grids covers from the Dominican Republic in the west and follows the Caribbean island chain to Antigua in the east. The north and south extents of the A-grid are designed to cover the deep ocean, especially the deep Puerto Rican trench found north of the island. This A grid is the same grid as used for the Charlotte Amalie, Virgin Islands forecast model developed at NCTR (Tolkova, in review). The Ponce forecast model B-grid covers all of the Puerto Rican island and is designed to capture the tsunami wave dynamics as they travel around the island. This is the same B-grid as used for the San Juan, Puerto Rico forecast model (Wei, in review). The highest resolution forecast grid, the Ponce C-grid focuses

in on Ponce and its bay. The goal of the higher resolution C-grids are to correctly describe tsunami wave heights and inundation in the shallow, complicated regions of the area where people live and work. The developed reference and forecast model grids are contoured in Figures 5 and 6 respectively.

4.0 Results and Discussion

The developed models are typically tested for accuracy and stability using a combination of historical and synthetic tsunami events. However, for Ponce and other Atlantic Ocean forecast models, data from historical events is not available. Therefore, the goal of model testing is to compare the fast-running forecast model to the high-resolution reference model and check that we have not lost important details or dynamics in the sub-sampling process of developing the forecast model. Further, to check that the forecast model is able to supply quality wave height estimates under strong forcing, a set of synthetic mega-tsunami events is used to test model stability.

4.1 Model Validation and Stability Testing

To test the stability and robustness of the forecast model, we use a set of 8 synthetic tsunamis. These events are 'synthetic' in the sense that they do not represent actual historical earthquakes, but allow us the flexibility to stress-test our model using large forcing inputs from many different directions. Of these test events, 6 are Mw 9.3 events that each use a set of 20 unit sources, corresponding to a rupture area of 1000 km by 100 km, and are located all around the Caribbean and Atlantic basins in each subduction zone. For a magnitude comparison, the 2004 Indian Ocean tsunami that resulted in hundreds of thousands of deaths in Indonesia, and was detectable globally, was the result of a Mw 9.1 earthquake. Tests, based on a local and remote medium sized events were also run to ensure that the model triggers correctly for low energy events. Table 2 describes the synthetic events used and their unit source combinations and Figure 7 shows the locations of these events and their positions relative to Ponce. The resulting maximum wave amplitude maps and time series of wave amplitudes at

8

the Ponce warning points as predicted from the forecast and reference models are shown in Figures 8 - 23. (When comparing events, note that the color maps and axes limits for these plots change from figure to figure.)

The first synthetic event discussed here originates on the Atlantic Source Zone from source blocks 38 to 47 (ATSZ38-47). This event is centered past the eastern arc of the Caribbean Islands of Martinique, and Antigua and Barbuda. The reference and forecast models' maximum wave height predictions are shown in Figure 8. Both models predict similar inundation patterns, but the forecast model shows maxima of 3 meters within the bay, while the reference model has heights of that scale east of Ponce's bay at the mouth of the Rio Bucana. The time series of wave amplitude at the warning point for this event (Figure 9) shows that the wave frequency and amplitudes predicted by the forecast and reference models are well matched, with maxima of 1.5 meters shown. The timing of the event is also well predicted here.

The ATSZ48-57 event is closer to Puerto Rico, centered to the north of the island on the Puerto Rico Trench. As you would expect, the magnitudes of the waves predicted are higher. Figure 10 shows that the reference and forecast models predict waves on the order of 6 meters. Once again, the forecast model shows higher amplitudes that the reference model, but both predict inundation of the same areas. Wave amplitude at the warning point (Figure 11) is approximately 3 meters at its highest, and tapers off 4 hours after the event.

The predictions for the ATSZ58-67 event are shown in Figures 12 and 13. This event is centered south of eastern Cuba and forces waves of over 1 meter at Ponce. The maxima maps for the forecast and reference models are very well matched. Inundation is seen in both models, but is limited to the low-lying areas near the coast. The time series shows that the predictions are almost exact for the initial waves, but the reference predicts higher heights past the second strong wave.

Figure 14 shows the maximum wave amplitudes for the ATSZ68-77 event, which are seen to be smaller and with minimal inundation. The timing of wave heights at the warning point (Figure 15) is well matched, but the reference model predicts slightly higher waves.

The largest waves predicted in the Ponce models result from the ATSZ82-91 synthetic event (Figure 16). This event is the closest to Ponce, and occurs on the fault line just to the south of Puerto Rico. Wave height maxima are over 6 meters in a large part of the model maps and extreme inundation is predicted. While, the patterns of wave maxima predicted by the forecast model matches the reference model, the forecast model predicts higher waves. The time-series at the warning point shown in Figure 17 shows wave heights topping 3 meters in both models and that the differences between maximum values predicted are smaller at this location.

The last mega-tsunami synthetic case is the SSSZ01-10 event, shown in Figure 18. This source zone, the South Sandwich Islands Source Zone, is in the southern Atlantic. This results in smaller, yet still significant wave heights at Ponce. For this event, the reference model predicts wave heights of over 20 centimeters in all of Ponce's bay and in the eastern edges of the grid domain.

Both the local and remote medium synthetic events (Figures 20 - 23) show minimal and negligible response at Ponce. This result is still important in that it shows that the forecast model will correctly trigger and predict events with very low energy. Finally and most importantly, note that for all the synthetic events tested, the forecast model developed here for Ponce is stable under extreme forcing.

5.0 Summary and Conclusions

We have developed a set of optimized and reference tsunami forecast models for Ponce, Puerto Rico. The models have been validated and stress-tested using synthetic mega, medium and micro tsunami events. The grid developed for the forecast model has resolutions in longitude and latitude of 1 arc-second – corresponding to a grid spacing of approximately 30 meters. Four hours of model time can be run in approximately 12 minutes, and is capable of providing fast wave height estimates during a real-time event.

The models give accurate predictions of wave height and water velocity in response to tsunami forcing. These models are part of NOAA's tsunami forecast and warning system and will be used to predict, in real-time, the potential threat of tsunami waves for the people and resources of the community of Ponce.

6.0 Acknowledgments

7.0 References

Gica, E., M. Spillane, V.V. Titov, C. Chamberlin, and J.C. Newman (2008): Development of the forecast propagation database for NOAA's Short-term Inundation Forecast for Tsunamis (SIFT). NOAA Tech. Memo. OAR PMEL-139, 89 pp.

Marks, K.M., and Smith, W.H.F. (2006): An evaluation of publicly available global bathymetry grids. Marine Geophysical Research, 27, 19-34.

Synolakis, C.E., E.N. Bernard, V.V. Titov, U.Kanoglu and F. Gonzalez (2008). Validation and verification of tsunami numerical models. *Pure Appl. Geophys.*, *165*(11–12), 2197–2228.

Tang, L., V. V. Titov, and C. D. Chamberlin (2009), Development, testing, and applications of site-specific tsunami inundation models for real-time forecasting, J. Geophys. Res., 114, C12025, doi:10.1029/2009JC005476.

Tang, L.J., Chamberlin, C., Titov, V.V. and Tolkova, E. (2006): A Stand-by Inundation Model f Kahului, Hawaii for NOAA Short-term Inundation Forecasting For Tsunamis (SIFT). NOAA Tech. Memo. OAR PMEL-XXX, 56p.

Taylor, L.a., B.W. Eakins, K.S Carignan, R.R. Warnken, T. Sazonova and D.C. Schoolcraft (2007): Digital elevation models for Puerto Rico: Procedures, data sources and analysis. NOAA Technical Memorandum NESDIS NGDC-13, US Dept. of Commerce, Boulder CO, 27 pp.

Titov, V.V. (2009): Tsunami forecasting. Chapter 12 in *The Sea, Volume 15: Tsunamis*, Harvard University Press, Cambridge, MA and London, England, 371–400.

Titov, V.V., Gonzalez, F.I., Bernard, E.N., Eble, M.C., Mofjeld, H.O., Newman, J.C. and Venturato, A.J. (2005). Real-time tsunami forecasting: challenges and solutions. Natural Hazards, 35(1), 41-58.

Tolkova, E. (in review): A Tsunami Forecast Model for Charlotte Amalie, Virgin Islands. NOAA OAR Special Report, PMEL Tsunami Forecast Series.

Wei, Y. (in review): A Tsunami Forecast Model for San Juan, Puerto Rico. NOAA OAR Special Report, PMEL Tsunami Forecast Series.

Wei, Y, E. N. Bernard, L. Tang, R. Weiss, V.V. Titov, C. Moore, M. Spillane, M. Hopkins and U. Kanoglu (2008): Real-time experimental forecast of the Peruvian tsunami of August 2007 for U.S. coastlines. *Geophys. Res. Lett.*, *35*, L04609, doi: 10.1029/2007GL032250.

Tables

Table 1: MOST setup parameters for reference and forecast models for Ponce, Puerto Rico.

		Reference Model				Forecast Model			
Grid	Region	Coverage Lat. [ºN] Lon. [ºE]	Cell Size ["]	nx x ny	Time Step [sec]	Coverage Lat. [º N] Lon. [ºE]	Cell Size ["]	nx x ny	Time Step [sec]
A	Caribbean	16.05 – 18.95 -69.9 – -60.504	20 x 20	1614 x 523	2.0	16.5 – 18.95 -69.0 - 61.0081	45 x 45	610 x 197	4.8
B	Puerto Rico	17.8 – 18.6 -66.6775 – -66.55	4 x 4	1621 x 721	0.5	17.8 – 18.6 -67.35– -65.55	12 x 12	541 x 241	1.2
C	Ponce	43.958 – 44.052 -66.6775 – -66.596	0.33 x 0.33	881 x 552	0.5	17.950 – 18.0 -66.668 – -66.596	1.0 x 1.0	260 x 180	1.2
Minimum offshore depth [m]		5				5			
Water depth for dry land [m]		0.1				0.1			
Friction coefficient [n^2]		0.0009				0.0009			
CPU time for 4-hr simulation		6.4 hr				12.7 min			

Computations were performed on a single Intel Xeon E5670 processor at 2.93 GHz, Dell PowerEdge R510.

Table 1 MOST model setup of the reference and forecast models for Ponce, Puerto Rico.

Sce. No	Scenario Name	Source Zone	Tsunami Source	α (m)
Mega-tsunami scenario				
1	ATSZ 38-47	Atlantic	A38-A47, A38-A47	25
2	ATSZ 48-57	Atlantic	A48-A57, B48-B57	25
3	ATSZ 58-67	Atlantic	A58-A67, B58-B67	25
4	ATSZ 68-77	Atlantic	A68-A77, B68-B77	25
5	ATSZ 82-91	Atlantic	A82-A91, B82-B91	25
6	SSSZ 1-10	South Sandwich	A1-A10, B1-B10	25
Mw 7.5 Scenario				
7	ATSZ B52	Atlantic	B52	1
Micro-tsunami Scenario				
8	SSSZ B11	South Sandwich	B11	5

Table 2 Unit source combinations used to generate synthetic mega-tsunami scenarios for robustness and stability testing of the Ponce forecast model.

Figures

Figure 1 Community tsunami evacuation map of Ponce. (Courtesy of the Puerto Rico Seismic Network)
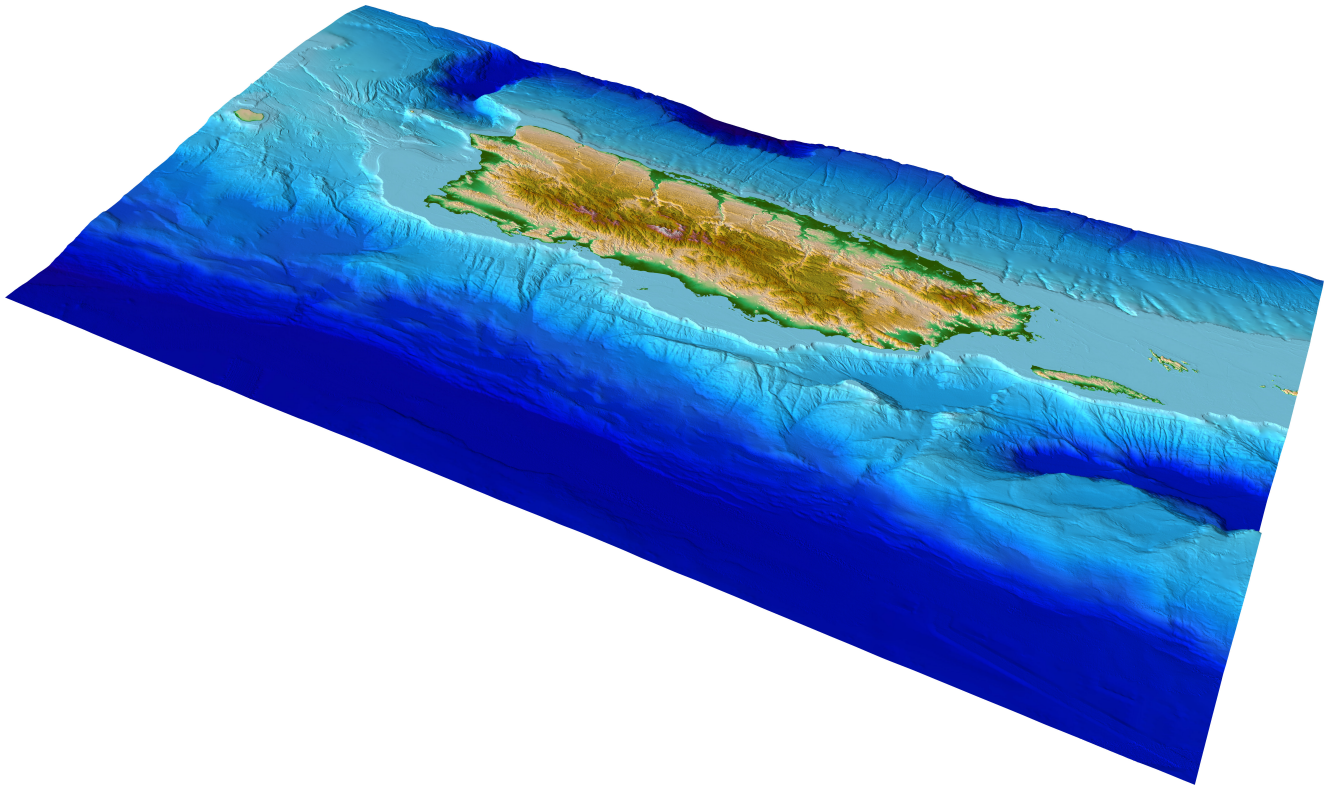
Figure 2 Perspective view of the 1 arc-second Puerto Rico digital elevation model developed by NGDC.

Figure 3 Aerial image of a Ponce. The marina and port are in the foreground while the majority of the city is in the middle and upper right of the photograph.
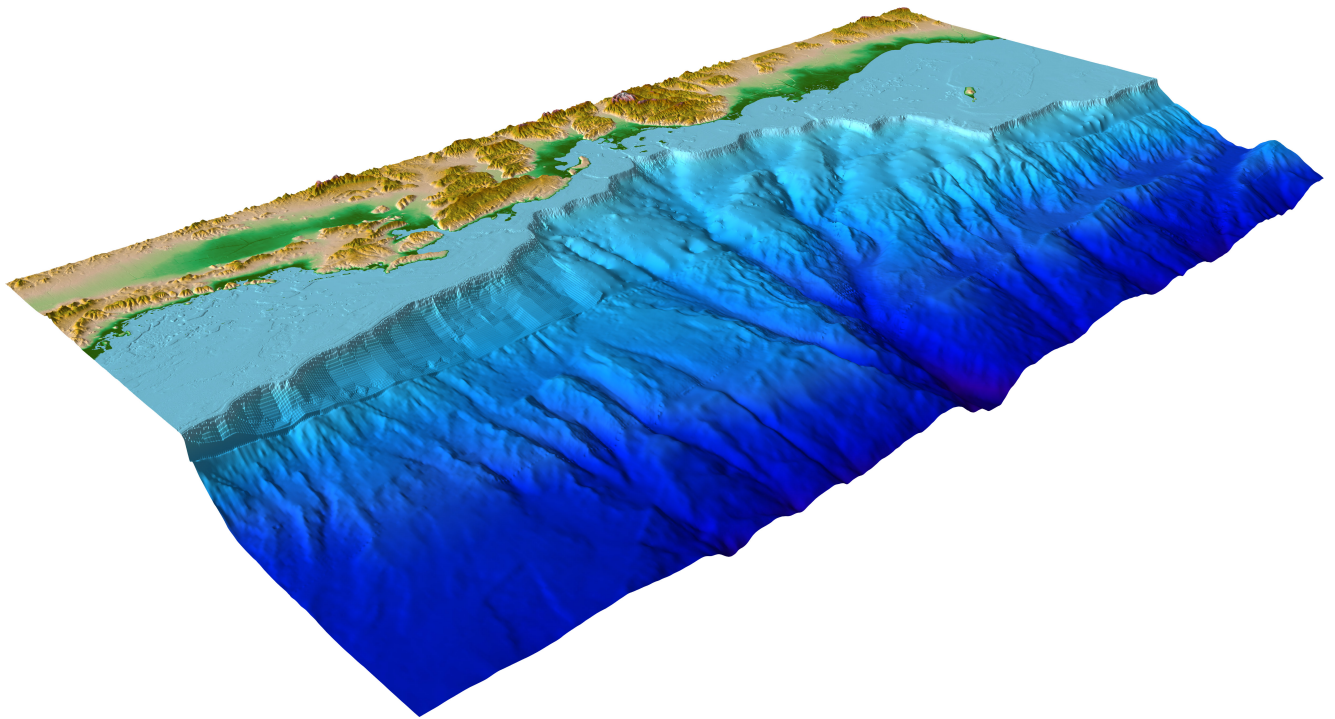
Figure 4 Bathymetry and topography map of the one-third arc-second digital elevation model for Ponce and the surrounding coast developed by NGDC.
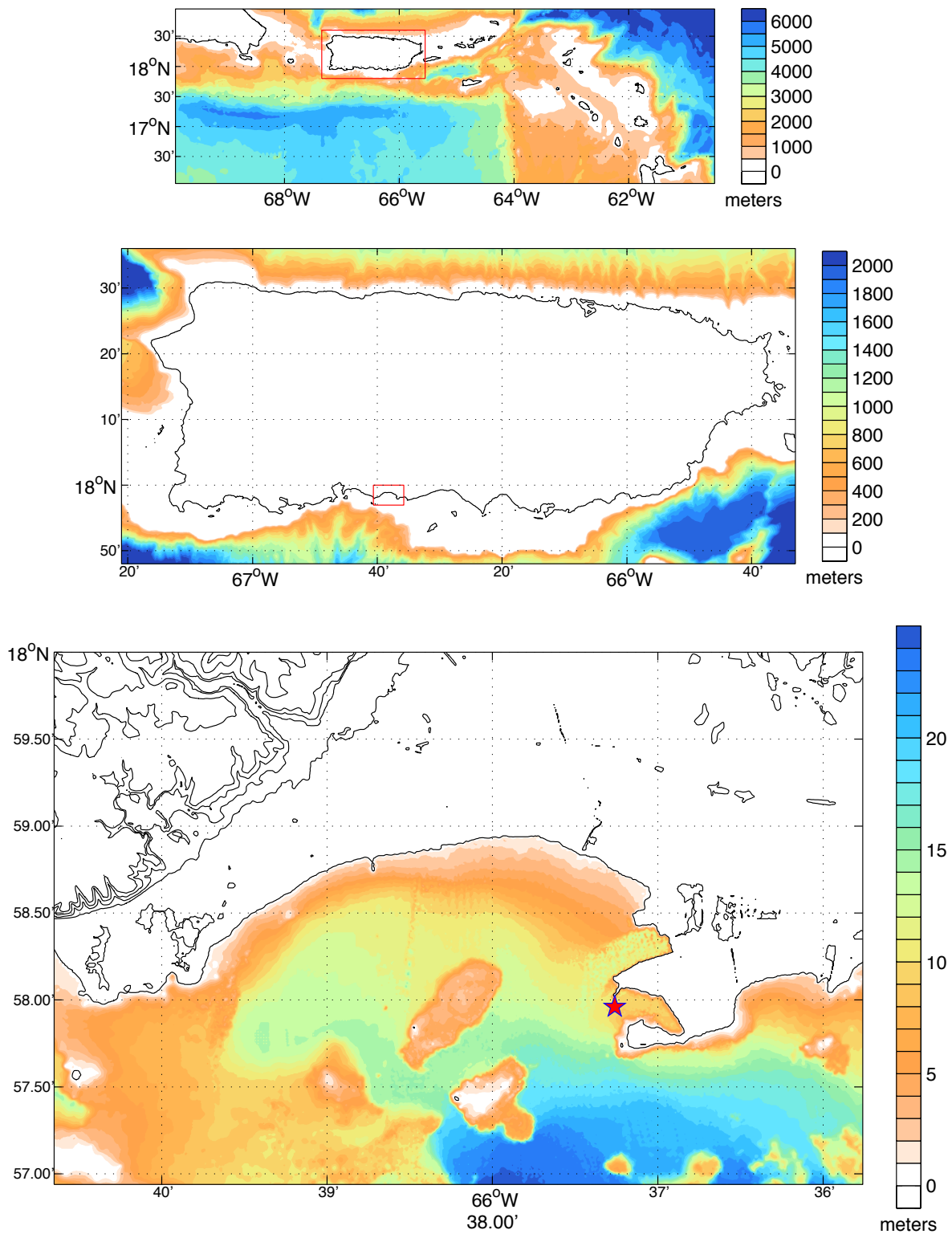
Figure 5 Bathymetry (meters) for the Ponce reference inundation model grids. The A grid is shown in the top panel, the B grid in the middle panel, and the C grid in the lower panel. The topography of the C grid is shown using contours with 10 meter intervals from 0 to 40 and then 40 meters intervals for higher values. The red boxes in the A and B plots show the position of the nested B and C grids, respectively.
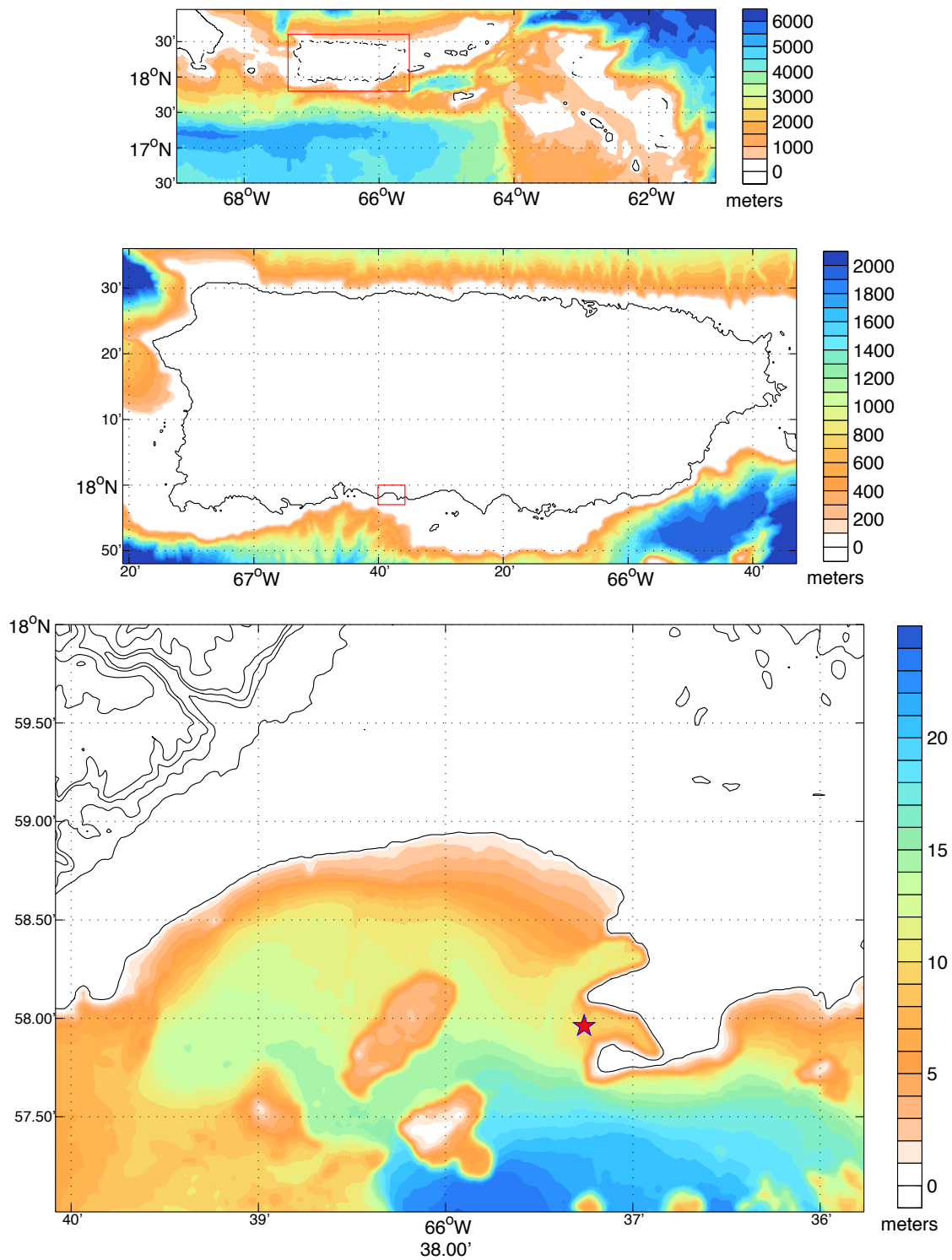
Figure 6 Bathymetry (meters) for the Ponce forecast inundation model grids. The A grid is shown in the top panel, the B grid in the middle panel, and the C grid in the bottom panel. The topography of the C grid is shown using contours with 10 meter intervals from 0 to 40 and then 40 meters intervals for higher values. The red boxes in the A and B plots show the position of the nested B and C grids, respectively. The red star shows the location of the Ponce warning point.
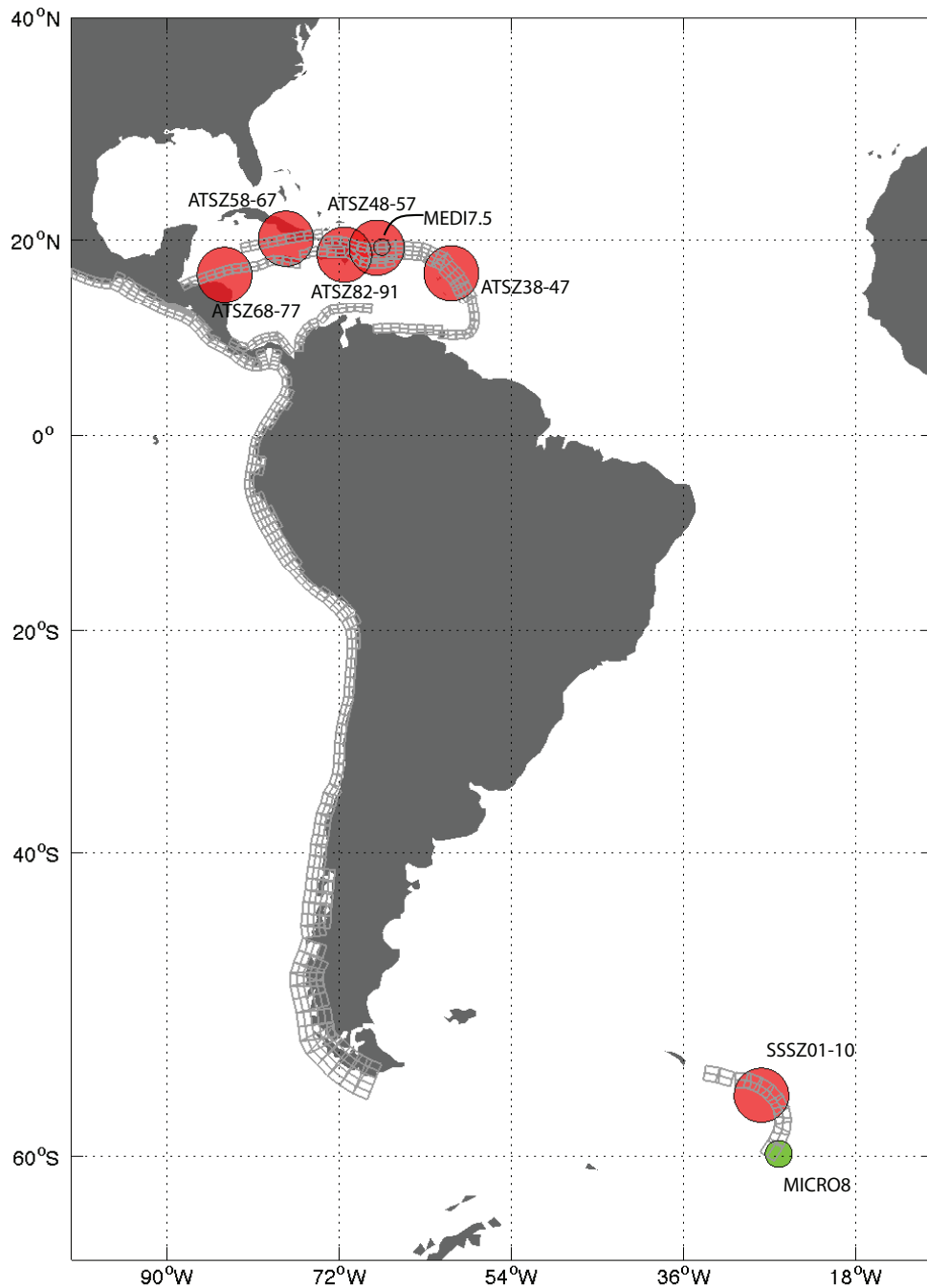
Figure 7 Map of the Caribbean and Atlantic Ocean Basins showing the locations of the 6 simulated Mw 9.3 events (red circles) and the medium (Mw 7.5, blue circle) and micro event (green circle) used to test and validate the Ponce model. The solid star denotes the location of Ponce.
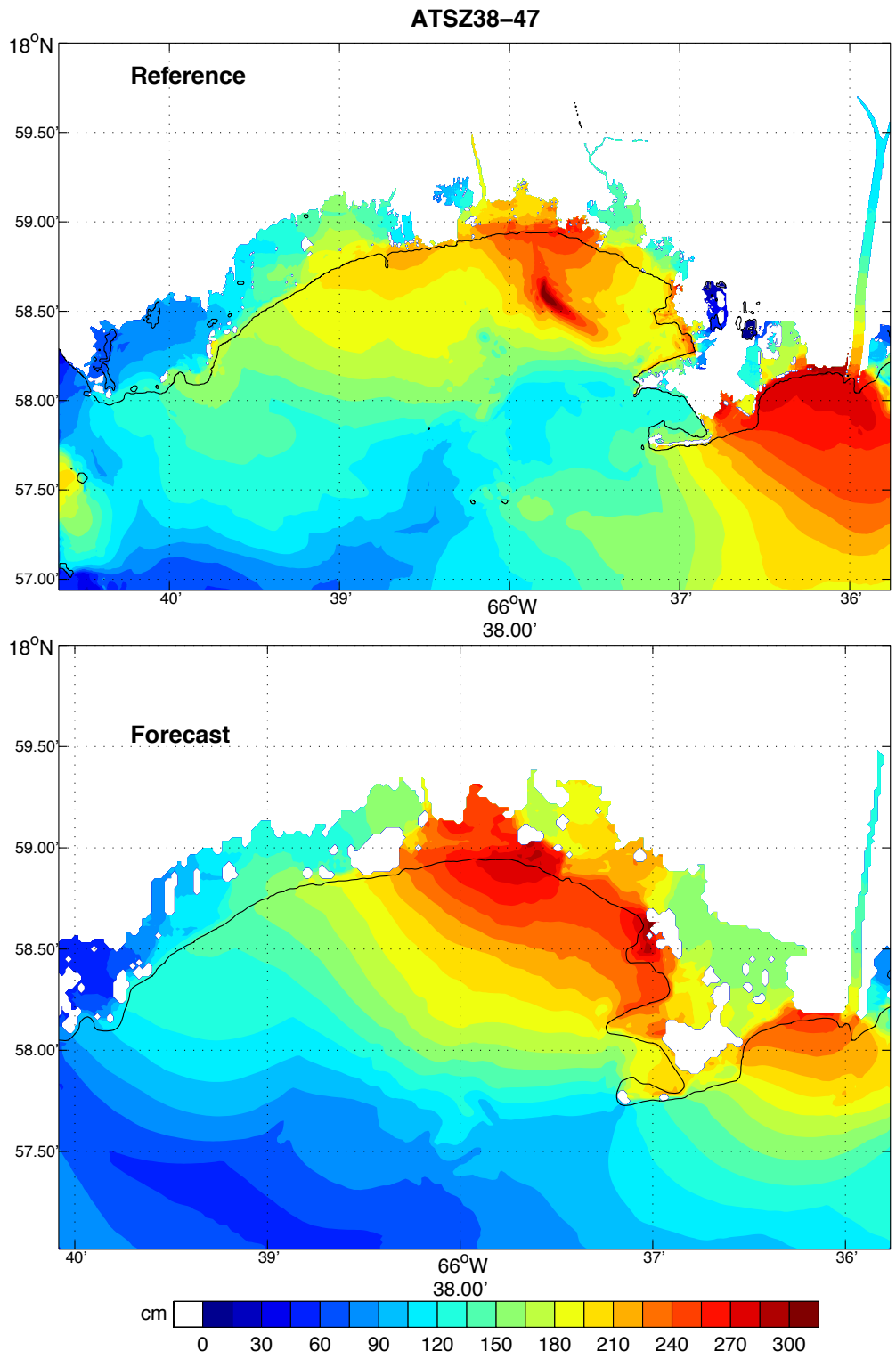
Figure 8 Results from the forecast model for the ATSZ 38-47 synthetic event. The upper panel shows the map of predicted maximum wave height in the Ponce reference model C-grid and the lower panel shows same data from the forecast model.
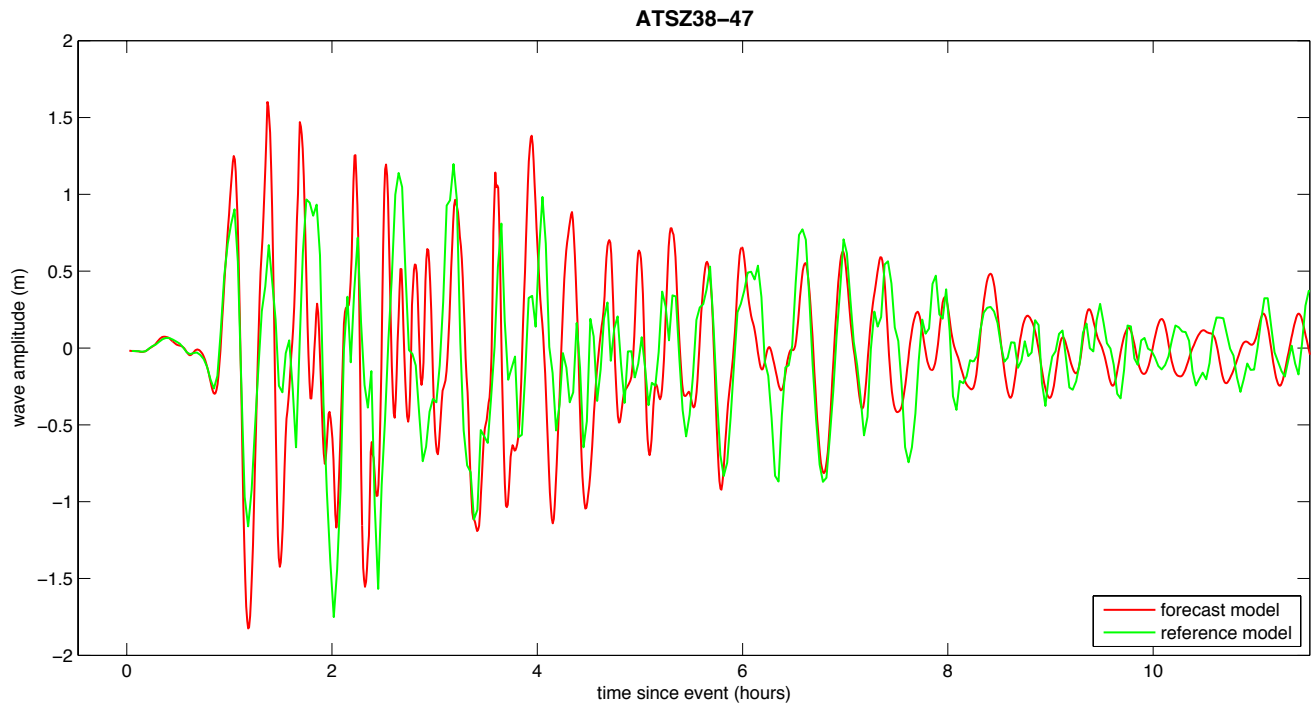
Figure 9 The time series of wave amplitude forced by the ATSZ 38-47 event at the Ponce warning point location from the reference (green) and forecast (red) models.

Figure 10 Results from the forecast model for the ATSZ 48-57 synthetic event. The upper panel shows the map of predicted maximum wave height in the Ponce reference model C-grid and the lower panel shows same data from the forecast model.

ATSZ48–57

Figure 11 The time series of wave amplitude forced by the ATSZ 48-57 event at the Ponce warning point location from the reference (green) and forecast (red) models.
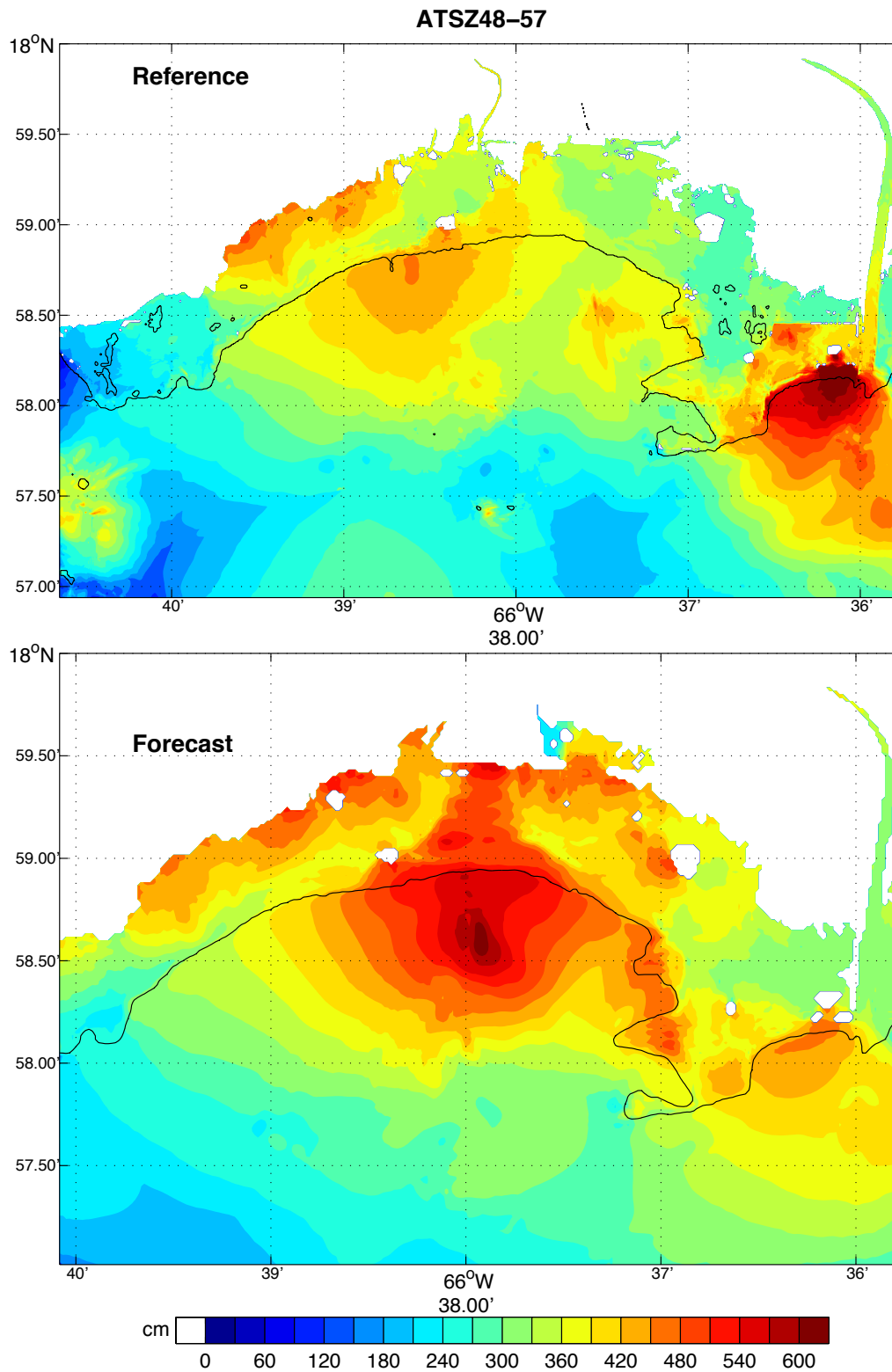
Figure 12 Results from the forecast model for the ATSZ 58-67 synthetic event. The upper panel shows the map of predicted maximum wave height in the Ponce reference model C-grid and the lower panel shows same data from the forecast model.

Figure 13 The time series of wave amplitude forced by the ATSZ 58-67 event at the Ponce warning point location from the reference (green) and forecast (red) models.

Figure 14 Results from the forecast model for the ATSZ 68-77 synthetic event. The upper panel shows the map of predicted maximum wave height in the Ponce reference model C-grid and the lower panel shows same data from the forecast model.
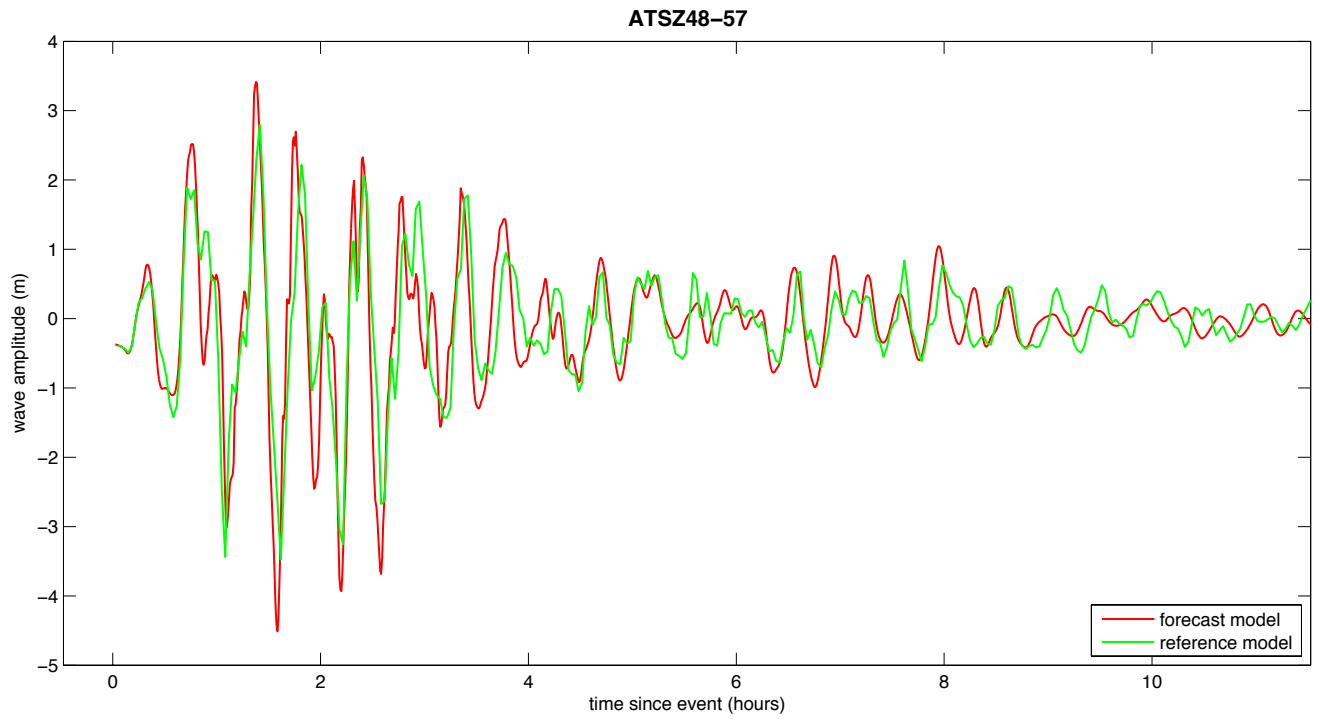
Figure 15 The time series of wave amplitude forced by the ATSZ 68-77 event at the Ponce warning point location from the reference (green) and forecast (red) models.
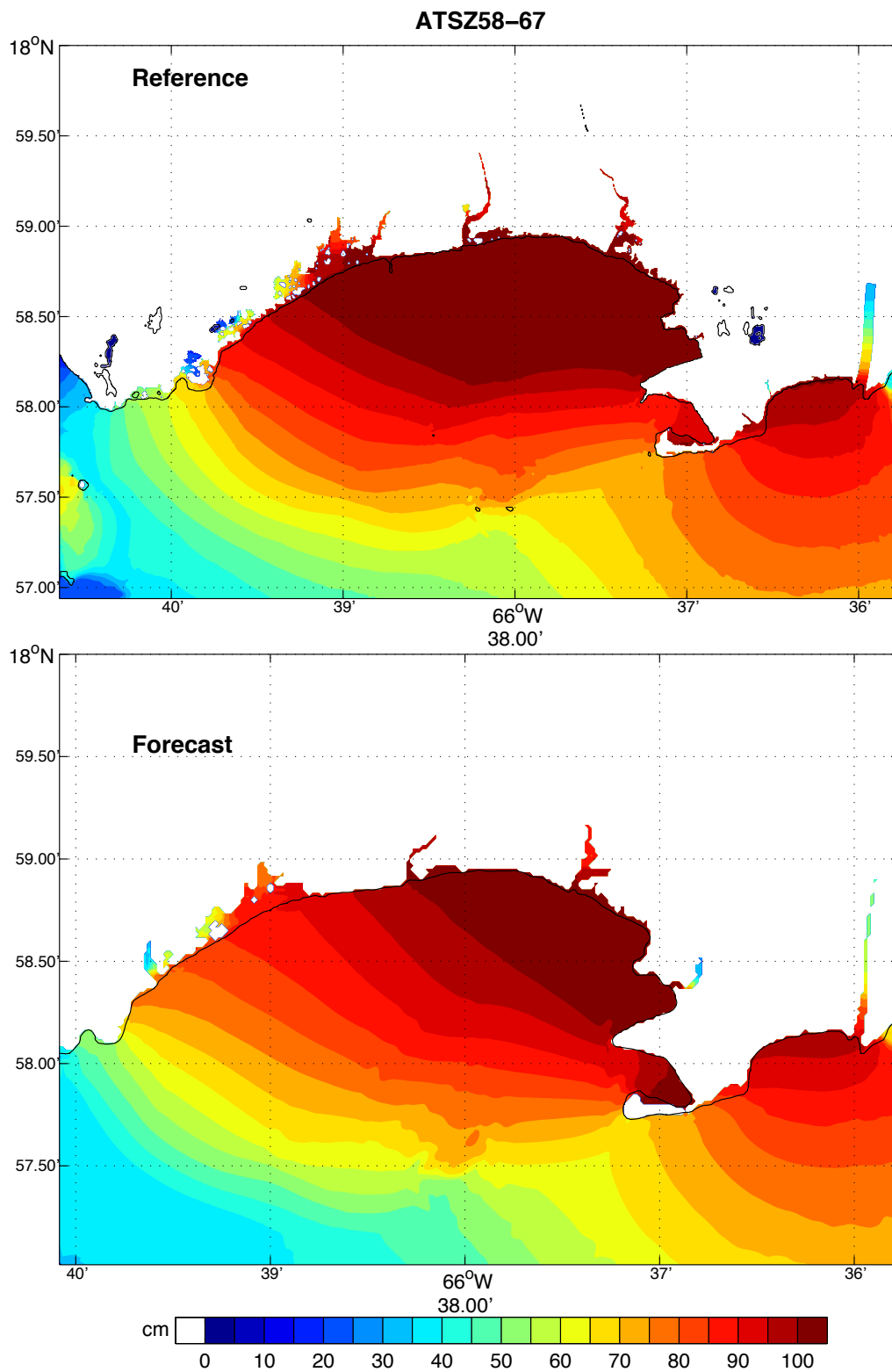
Figure 16 Results from the forecast model for the ATSZ 82-91 synthetic event. The upper panel shows the map of predicted maximum wave height in the Ponce reference model C-grid and the lower panel shows same data from the forecast model.
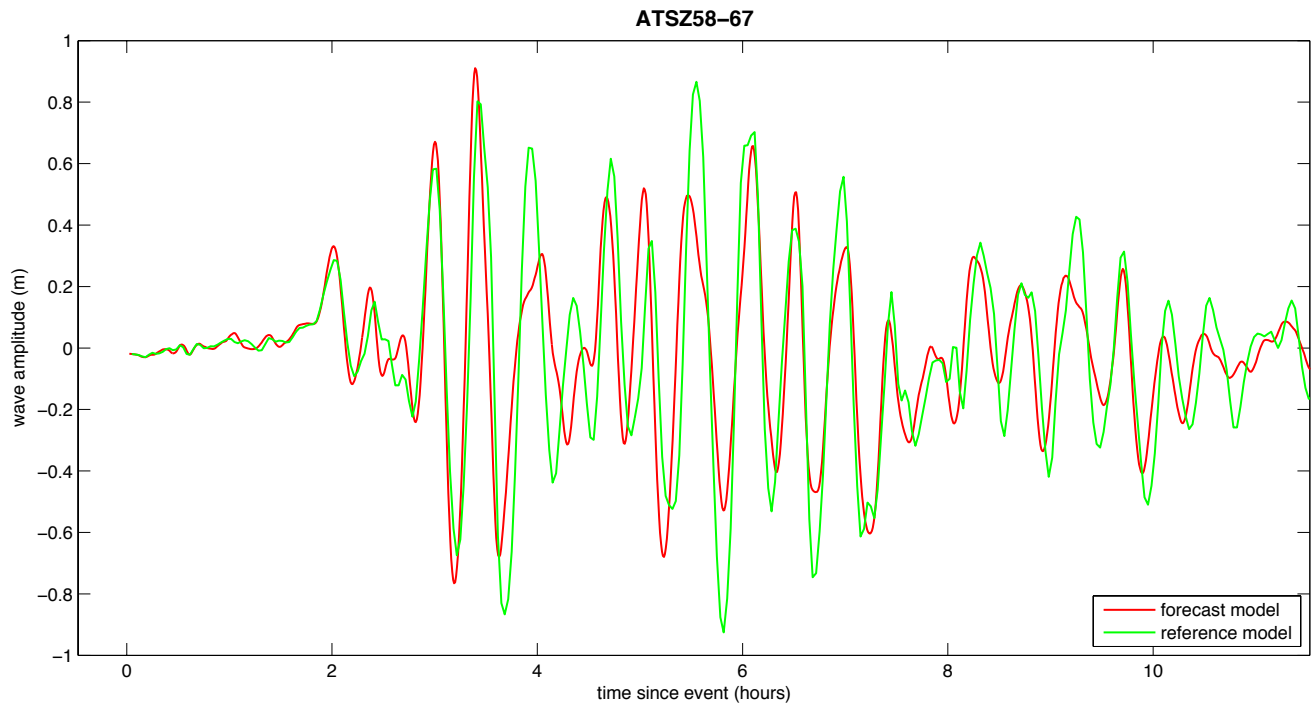
Figure 17 The time series of wave amplitude forced by the ATSZ 82-91 event at the Ponce warning point location from the reference (green) and forecast (red) models.
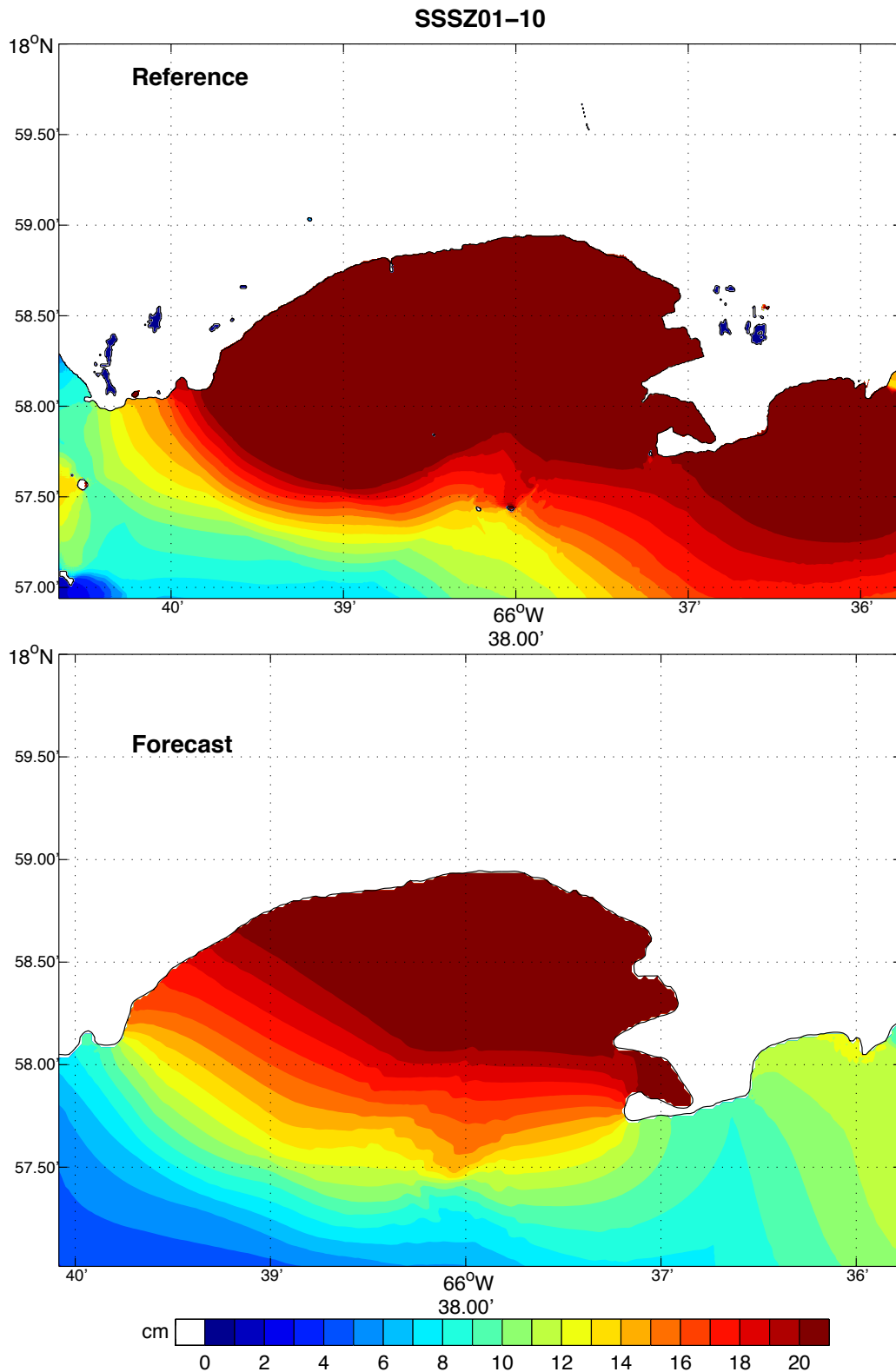
Figure 18 Results from the forecast model for the SSSZ 1-10 synthetic event. The upper panel shows the map of predicted maximum wave height in the Ponce reference model C-grid and the lower panel shows same data from the forecast model.

SSSZ01−10
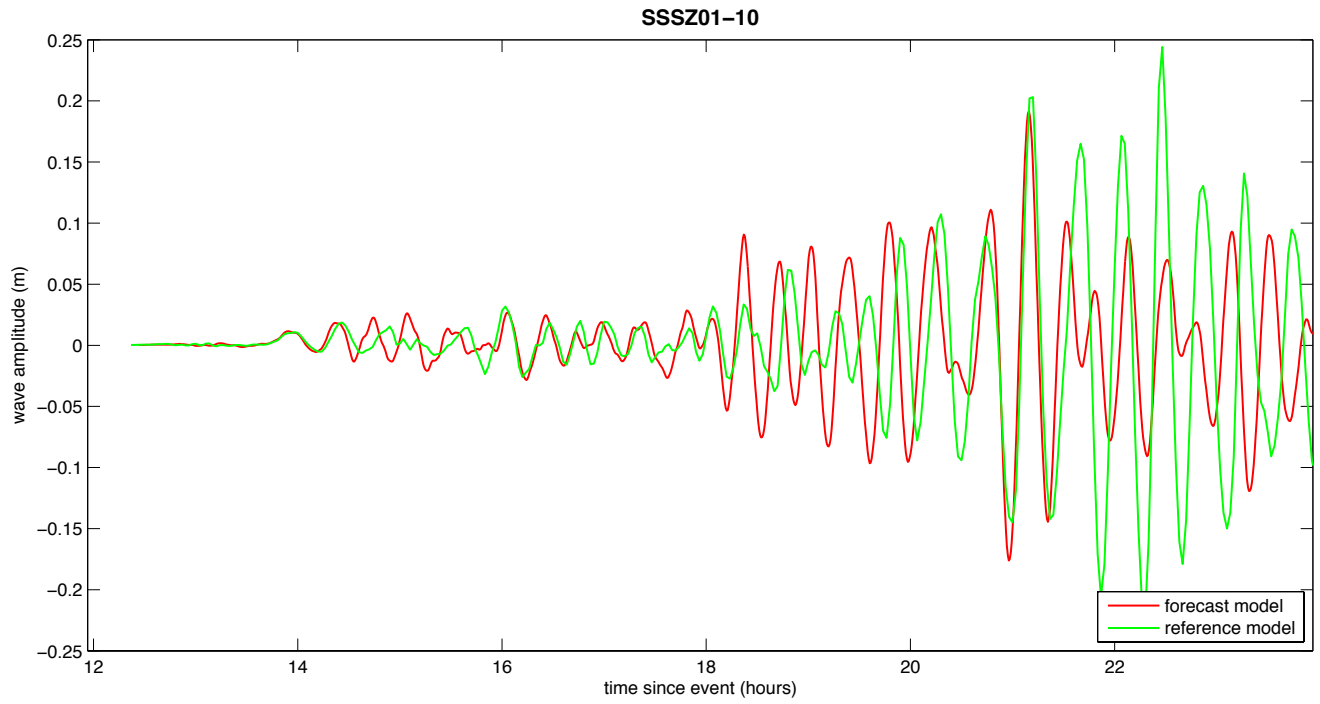
Figure 19 The time series of wave amplitude forced by the SSSZ 1-10 event at the Ponce warning point location from the reference (green) and forecast (red) models.
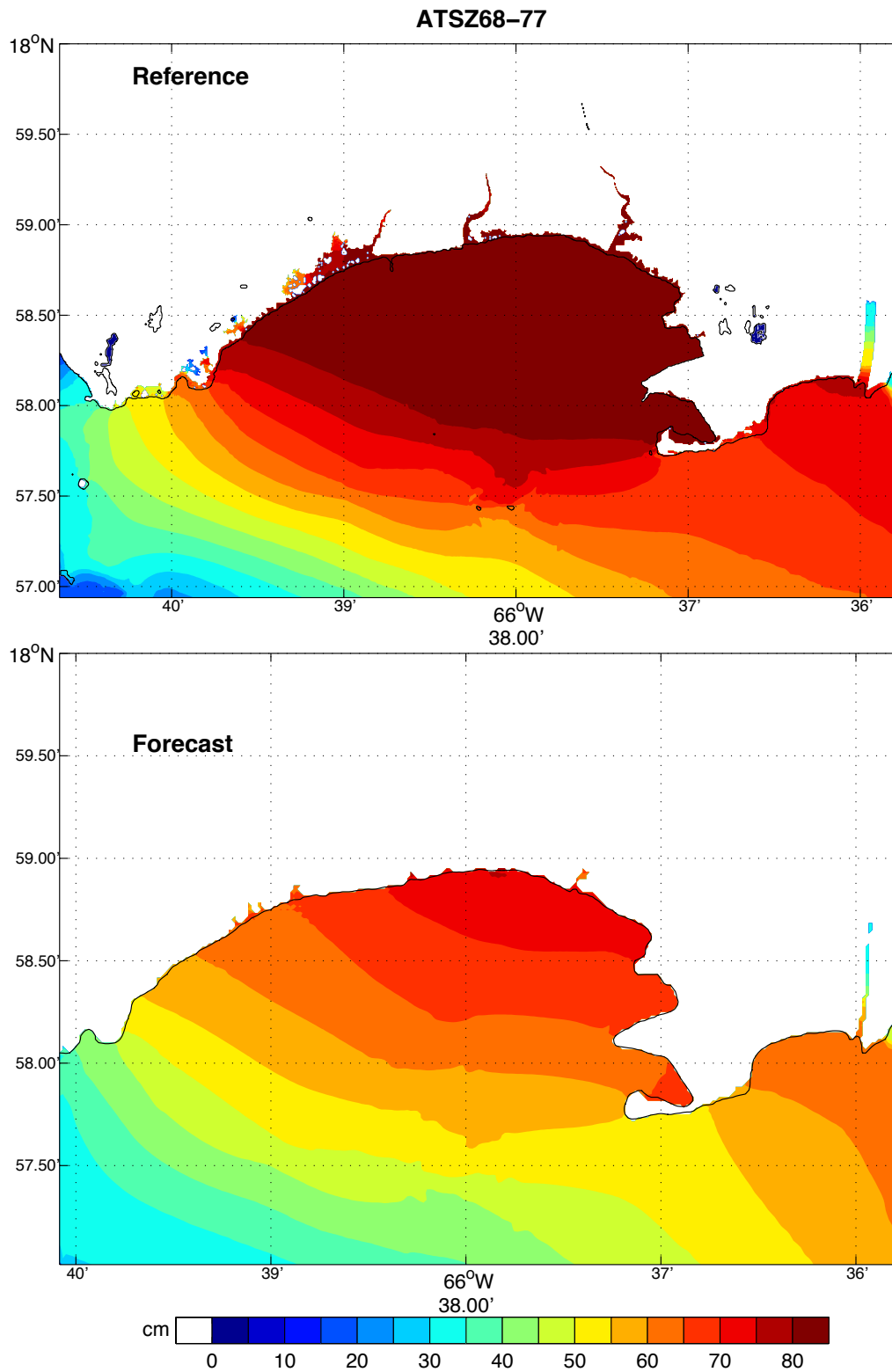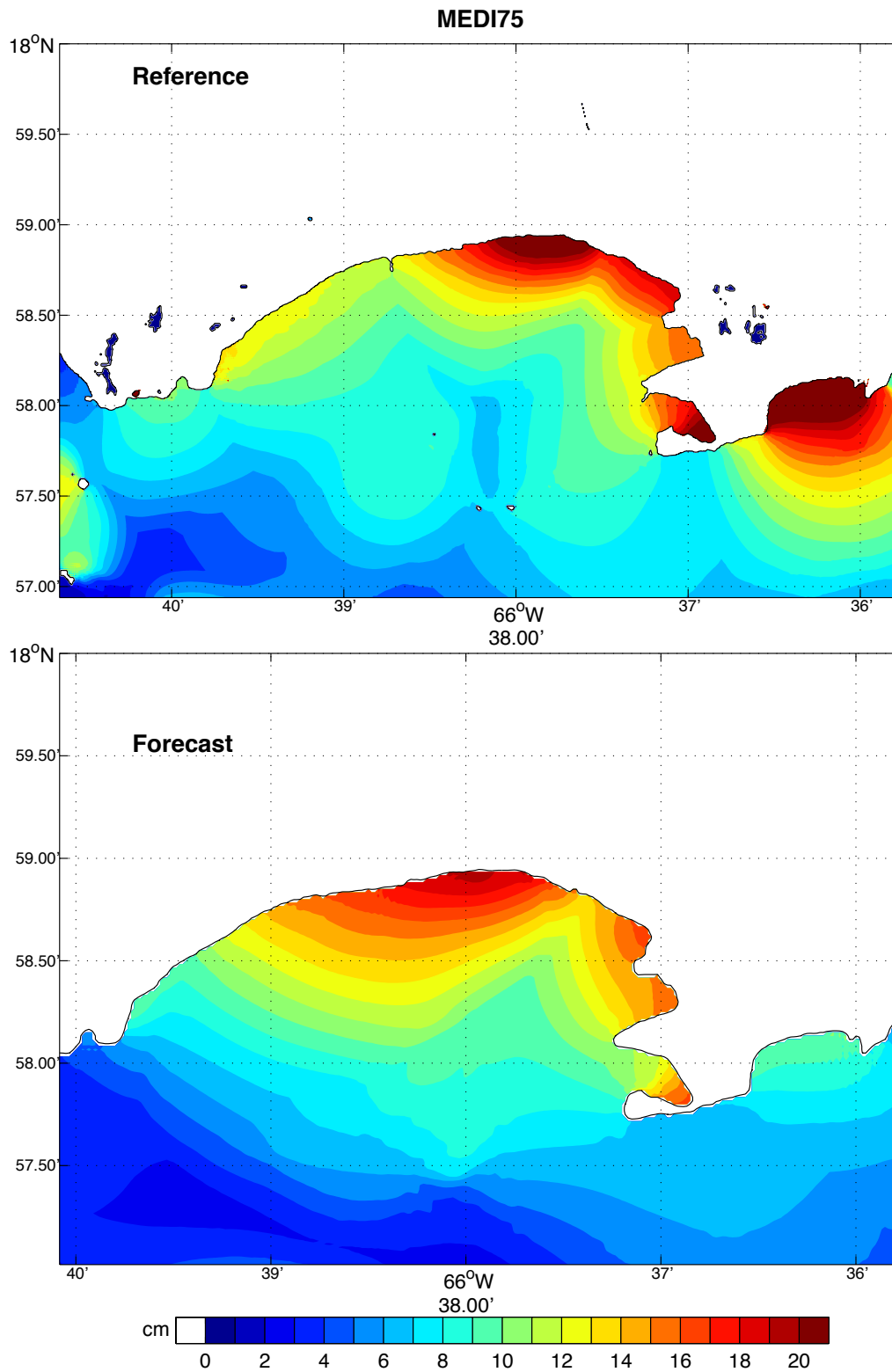
Figure 20 Results from the forecast model for the ATSZ B52 medium synthetic event. The upper panel shows the map of predicted maximum wave height in the Ponce reference model C-grid and the lower panel shows same data from the forecast model.
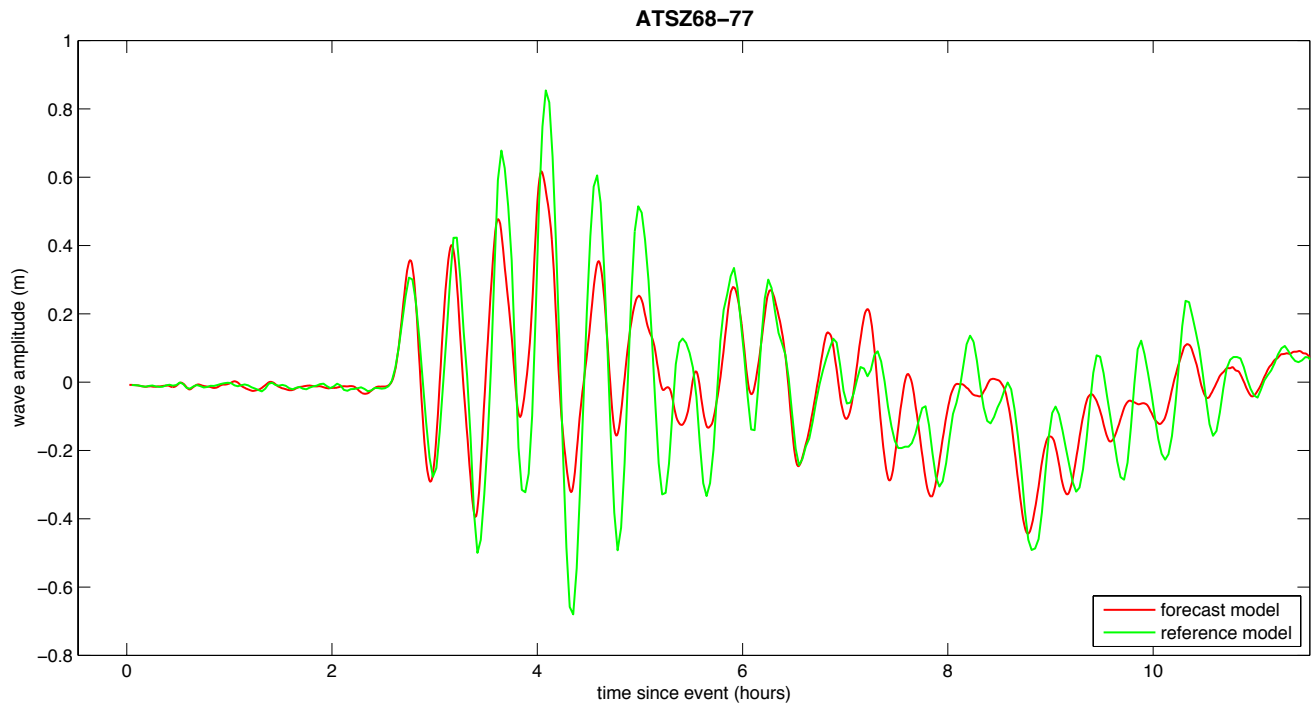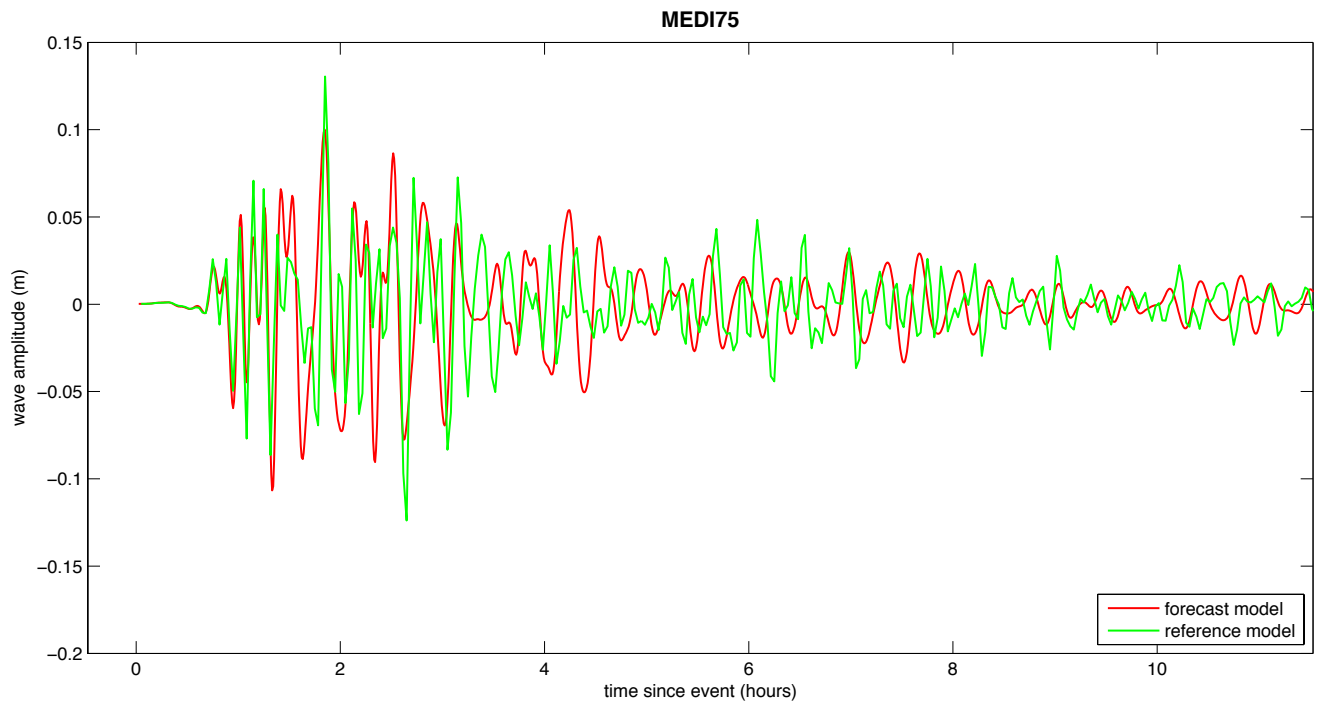
Figure 21 The time series of wave amplitude forced by the ATSZ B52 medium event at the Ponce warning point location from the reference (green) and forecast (red) models.
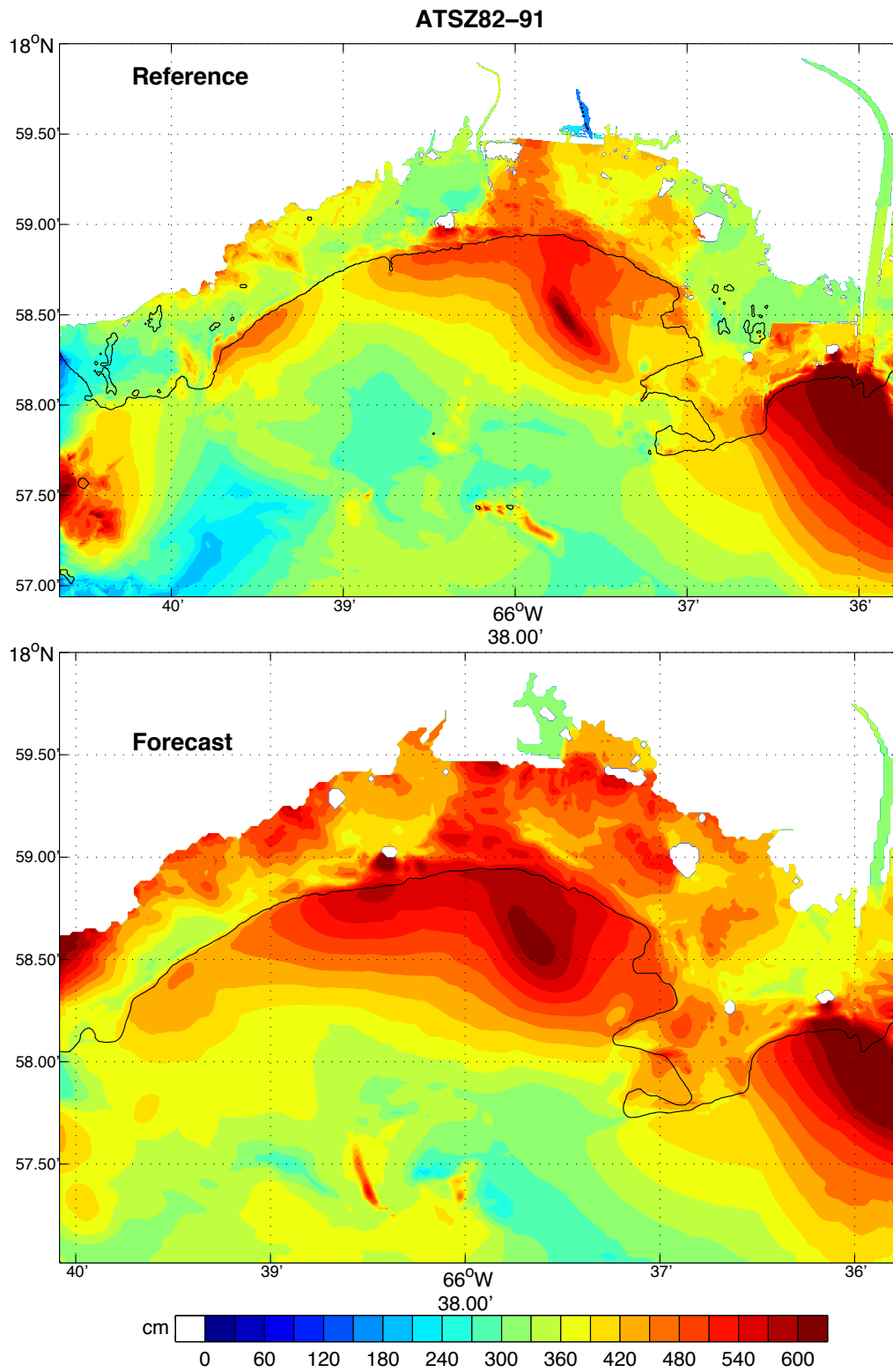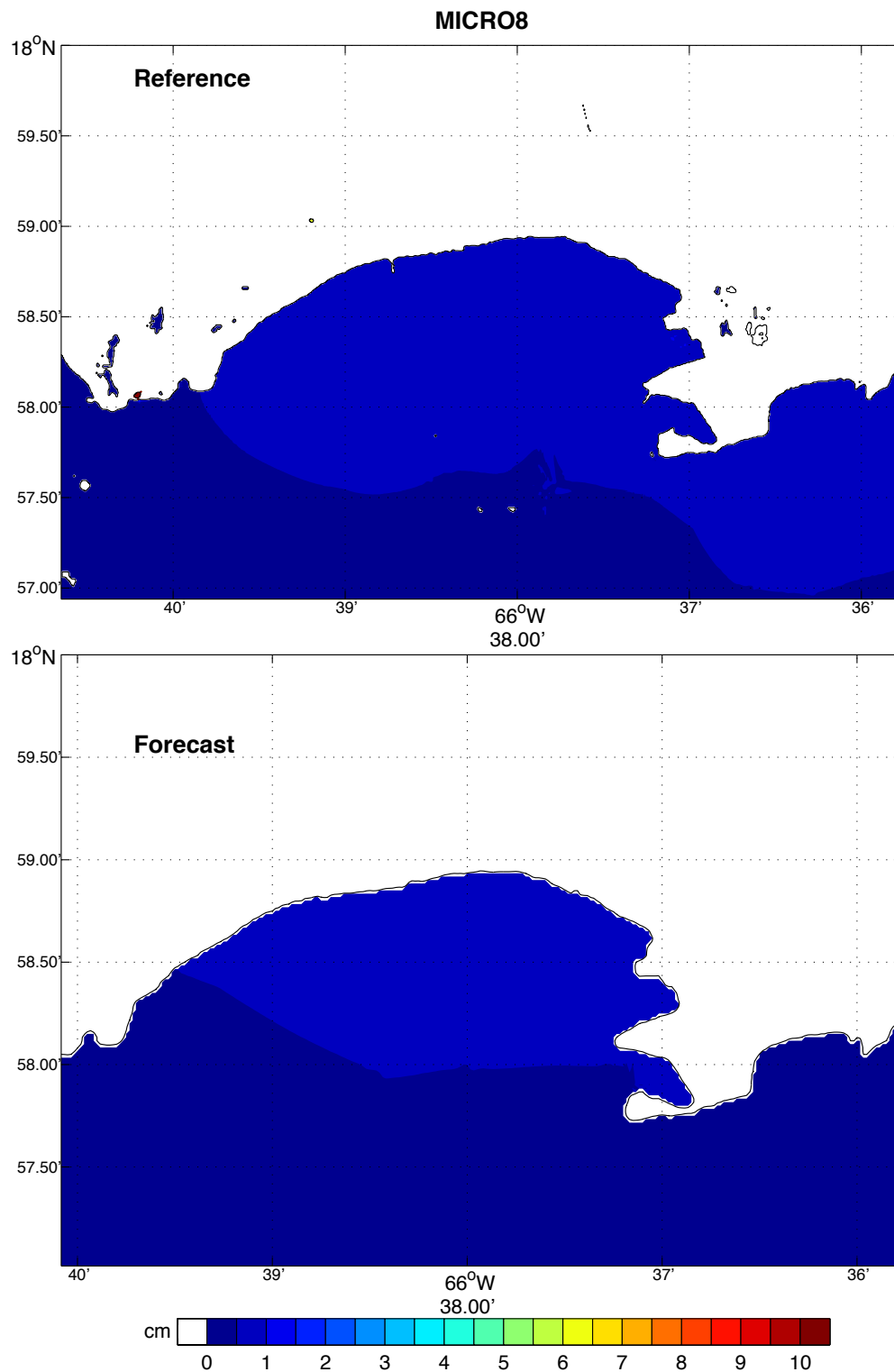
Figure 22 Results from the forecast model for SSSZ B11 synthetic event. The upper panel shows the map of predicted maximum wave height in the Florence C-grid and the lower panel shows the time series of wave amplitude at the warning point location.
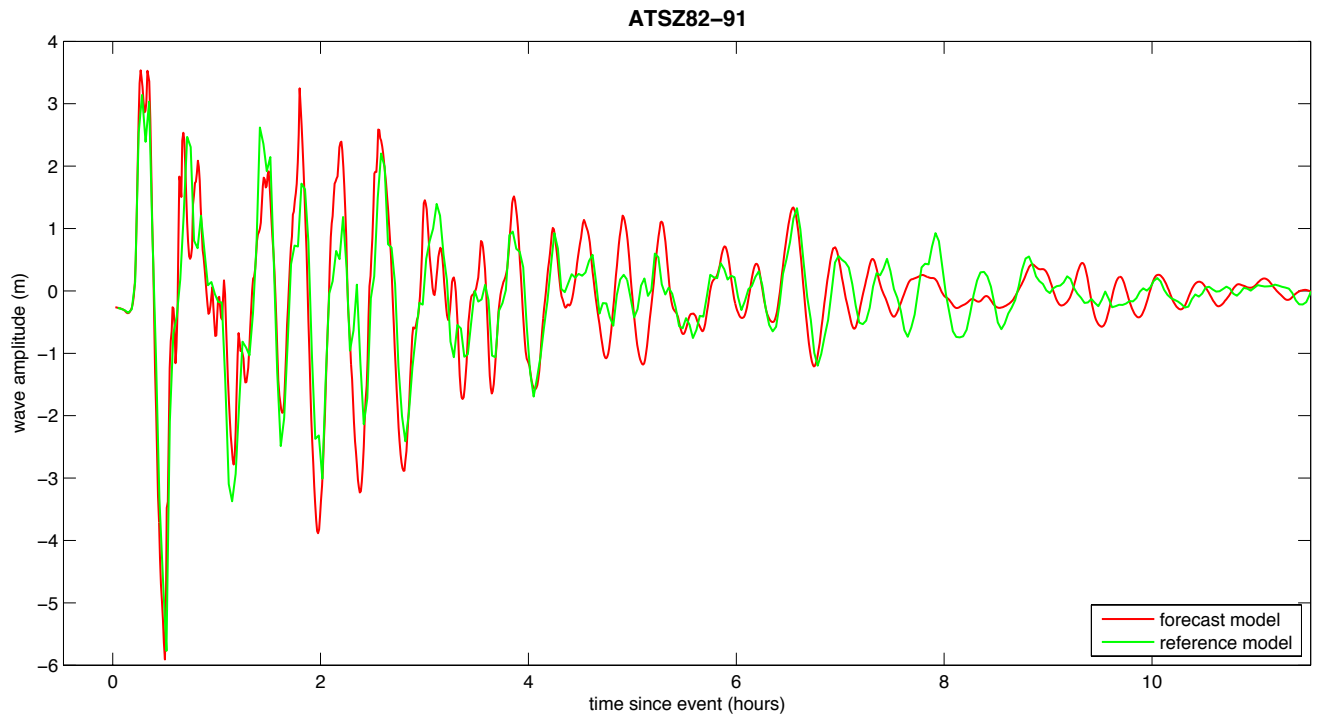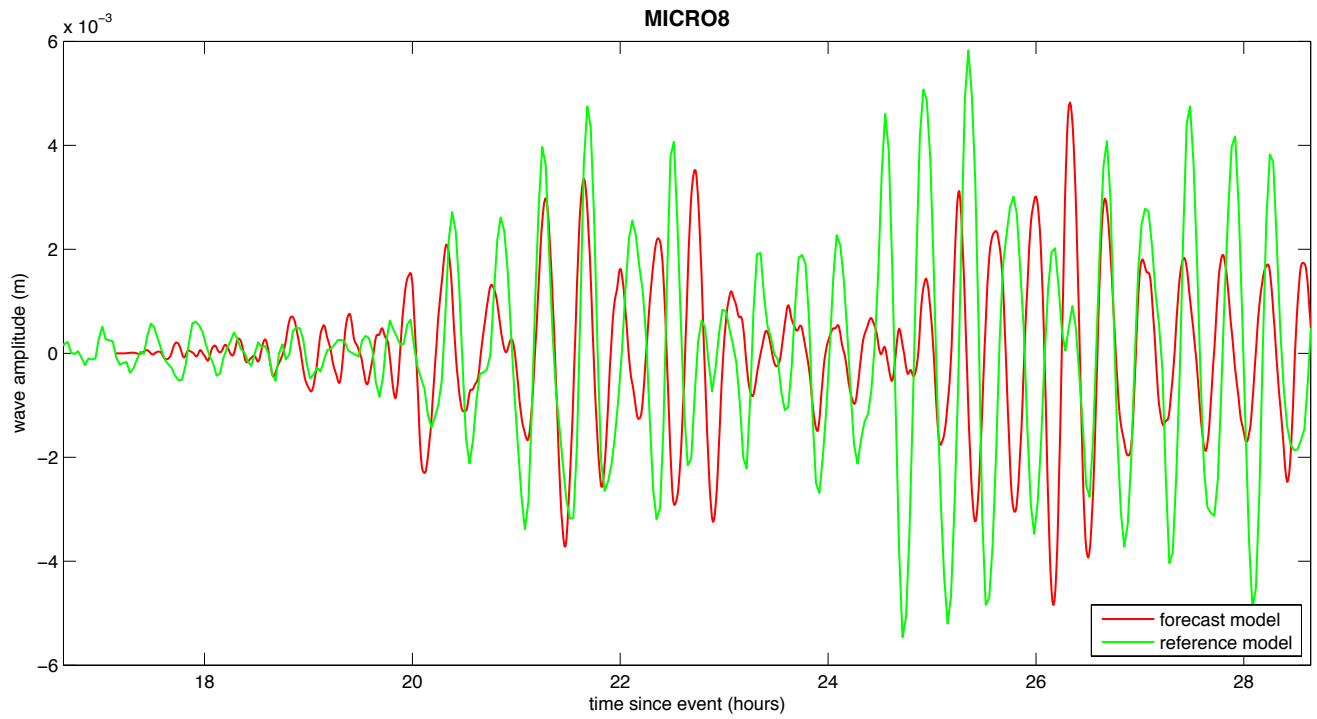
Figure 23 The time series of wave amplitude forced by the SSSZ B11 event at the Ponce warning point location from the reference (green) and forecast (red) models.

Appendix A

A.1 Reference model *.in file

```
0.001     Minimum amplitude of input offshore wave (m):
5    Input minimum depth for offshore (m)
0.1  Input "dry land" depth for inundation (m)
0.0009      Input friction coefficient (n**2)
1        let a and b run up
500.0    max eta before blow up (m)
0.4  Input time step (sec)
172800     Input amount of steps
4    Compute "A" arrays every n-th time step, n=
1    Compute "B" arrays every n-th time step, n=
300  Input number of steps between snapshots
0    ...Starting from
1    ...Saving grid every n-th node, n=
0000Template/Anew20s_1nd_SSL1.9sm.asc.1nod
0000Template/ponceRB_7.most
0000Template/ponceRC_3.most
```

A.2 Forecast Model *.in file

```
0.001     Minimum amplitude of input offshore wave (m):
5    Input minimum depth for offshore (m)
0.1  Input "dry land" depth for inundation (m)
0.0009      Input friction coefficient (n**2)
1        let a and b run up
500.0    max eta before blow up (m)
1.2  Input time step (sec)
36000      Input amount of steps
4    Compute "A" arrays every n-th time step, n=
1    Compute "B" arrays every n-th time step, n=
28   Input number of steps between snapshots
0    ...Starting from
1    ...Saving grid every n-th node, n=
0000Template/A5_45s_SSL1.9_v2.asc
0000Template/SJ_grid_B_3
0000Template/ponceSC_11.most
```

Appendix B

Propagation Database: Atlantic Ocean Unit Sources

Figure B.1: Atlantic Source Zone unit sources.

Table B.1: Earthquake parameters for Atlantic Source Zone unit sources.

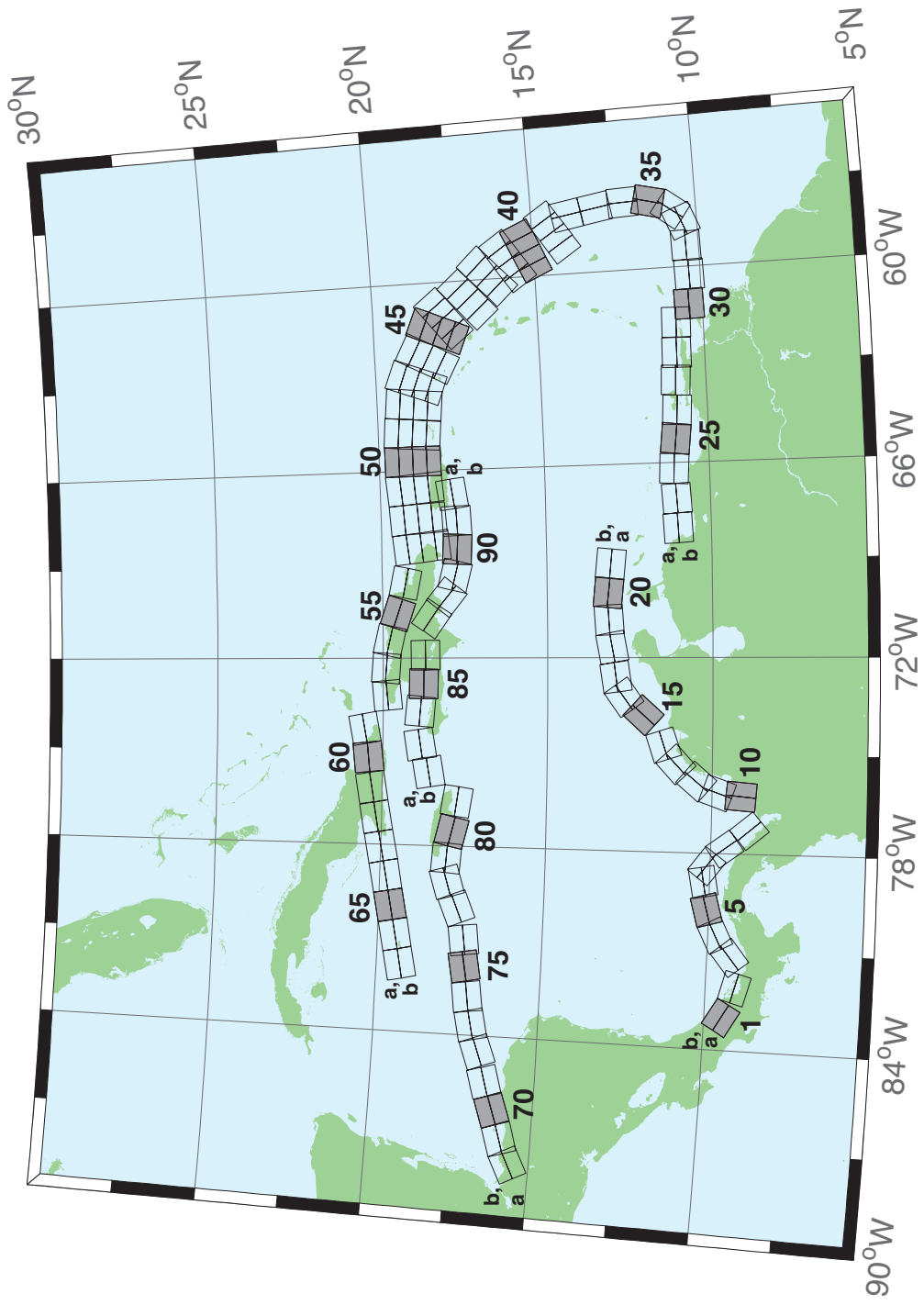| Segment	Description	Longitude(°E)	Latitude(°N)	Strike(°)	Dip(°)	Depth (km)
atsz–1a	Atlantic Source Zone	-83.2020	9.1449	120	27.5	28.09
atsz–1b	Atlantic Source Zone	-83.0000	9.4899	120	27.5	5
atsz–2a	Atlantic Source Zone	-82.1932	8.7408	105.1	27.5	28.09
atsz–2b	Atlantic Source Zone	-82.0880	9.1254	105.1	27.5	5
atsz–3a	Atlantic Source Zone	-80.9172	9.0103	51.31	30	30
atsz–3b	Atlantic Source Zone	-81.1636	9.3139	51.31	30	5
atsz–4a	Atlantic Source Zone	-80.3265	9.4308	63.49	30	30
atsz–4b	Atlantic Source Zone	-80.5027	9.7789	63.49	30	5
atsz–5a	Atlantic Source Zone	-79.6247	9.6961	74.44	30	30
atsz–5b	Atlantic Source Zone	-79.7307	10.0708	74.44	30	5
atsz–6a	Atlantic Source Zone	-78.8069	9.8083	79.71	30	30
atsz–6b	Atlantic Source Zone	-78.8775	10.1910	79.71	30	5
atsz–7a	Atlantic Source Zone	-78.6237	9.7963	127.2	30	30
atsz–7b	Atlantic Source Zone	-78.3845	10.1059	127.2	30	5
atsz–8a	Atlantic Source Zone	-78.1693	9.3544	143.8	30	30
atsz–8b	Atlantic Source Zone	-77.8511	9.5844	143.8	30	5
atsz–9a	Atlantic Source Zone	-77.5913	8.5989	139.9	30	30
atsz–9b	Atlantic Source Zone	-77.2900	8.8493	139.9	30	5
atsz–10a	Atlantic Source Zone	-75.8109	9.0881	4.67	17	19.62
atsz–10b	Atlantic Source Zone	-76.2445	9.1231	4.67	17	5
atsz–11a	Atlantic Source Zone	-75.7406	9.6929	19.67	17	19.62
atsz–11b	Atlantic Source Zone	-76.1511	9.8375	19.67	17	5
atsz–12a	Atlantic Source Zone	-75.4763	10.2042	40.4	17	19.62
atsz–12b	Atlantic Source Zone	-75.8089	10.4826	40.4	17	5
atsz–13a	Atlantic Source Zone	-74.9914	10.7914	47.17	17	19.62
atsz–13b	Atlantic Source Zone	-75.2890	11.1064	47.17	17	5
atsz–14a	Atlantic Source Zone	-74.5666	11.0708	71.68	17	19.62
atsz–14b	Atlantic Source Zone	-74.7043	11.4786	71.68	17	5
atsz–15a	Atlantic Source Zone	-73.4576	11.8012	42.69	17	19.62
atsz–15b	Atlantic Source Zone	-73.7805	12.0924	42.69	17	5
atsz–16a	Atlantic Source Zone	-72.9788	12.3365	54.75	17	19.62
atsz–16b	Atlantic Source Zone	-73.2329	12.6873	54.75	17	5
atsz–17a	Atlantic Source Zone	-72.5454	12.5061	81.96	17	19.62
atsz–17b	Atlantic Source Zone	-72.6071	12.9314	81.96	17	5
atsz–18a	Atlantic Source Zone	-71.6045	12.6174	79.63	17	19.62
atsz–18b	Atlantic Source Zone	-71.6839	13.0399	79.63	17	5
atsz–19a	Atlantic Source Zone	-70.7970	12.7078	86.32	17	19.62
atsz–19b	Atlantic Source Zone	-70.8253	13.1364	86.32	17	5
atsz–20a	Atlantic Source Zone	-70.0246	12.7185	95.94	17	19.62
atsz–20b	Atlantic Source Zone	-69.9789	13.1457	95.94	17	5
atsz–21a	Atlantic Source Zone	-69.1244	12.6320	95.94	17	19.62
atsz–21b	Atlantic Source Zone	-69.0788	13.0592	95.94	17	5
atsz–22a	Atlantic Source Zone	-68.0338	11.4286	266.9	15	17.94
atsz–22b	Atlantic Source Zone	-68.0102	10.9954	266.9	15	5
atsz–23a	Atlantic Source Zone	-67.1246	11.4487	266.9	15	17.94
atsz–23b	Atlantic Source Zone	-67.1010	11.0155	266.9	15	5
atsz–24a	Atlantic Source Zone	-66.1656	11.5055	273.3	15	17.94
atsz–24b	Atlantic Source Zone	-66.1911	11.0724	273.3	15	5
atsz–25a	Atlantic Source Zone	-65.2126	11.4246	276.4	15	17.94
atsz–25b	Atlantic Source Zone	-65.2616	10.9934	276.4	15	5
atsz–26a	Atlantic Source Zone	-64.3641	11.3516	272.9	15	17.94
atsz–26b	Atlantic Source Zone	-64.3862	10.9183	272.9	15	5
atsz–27a	Atlantic Source Zone	-63.4472	11.3516	272.9	15	17.94

Segment	Description	Longitude(°E)	Latitude(°N)	Strike(°)	Dip(°)	Depth (km)
atsz–27b	Atlantic Source Zone	-63.4698	10.9183	272.9	15	5
atsz–28a	Atlantic Source Zone	-62.6104	11.2831	271.1	15	17.94
atsz–28b	Atlantic Source Zone	-62.6189	10.8493	271.1	15	5
atsz–29a	Atlantic Source Zone	-61.6826	11.2518	271.6	15	17.94
atsz–29b	Atlantic Source Zone	-61.6947	10.8181	271.6	15	5
atsz–30a	Atlantic Source Zone	-61.1569	10.8303	269	15	17.94
atsz–30b	Atlantic Source Zone	-61.1493	10.3965	269	15	5
atsz–31a	Atlantic Source Zone	-60.2529	10.7739	269	15	17.94
atsz–31b	Atlantic Source Zone	-60.2453	10.3401	269	15	5
atsz–32a	Atlantic Source Zone	-59.3510	10.8123	269	15	17.94
atsz–32b	Atlantic Source Zone	-59.3734	10.3785	269	15	5
atsz–33a	Atlantic Source Zone	-58.7592	10.8785	248.6	15	17.94
atsz–33b	Atlantic Source Zone	-58.5984	10.4745	248.6	15	5
atsz–34a	Atlantic Source Zone	-58.5699	11.0330	217.2	15	17.94
atsz–34b	Atlantic Source Zone	-58.2179	10.7710	217.2	15	5
atsz–35a	Atlantic Source Zone	-58.3549	11.5300	193.7	15	17.94
atsz–35b	Atlantic Source Zone	-57.9248	11.4274	193.7	15	5
atsz–36a	Atlantic Source Zone	-58.3432	12.1858	177.7	15	17.94
atsz–36b	Atlantic Source Zone	-57.8997	12.2036	177.7	15	5
atsz–37a	Atlantic Source Zone	-58.4490	12.9725	170.7	15	17.94
atsz–37b	Atlantic Source Zone	-58.0095	13.0424	170.7	15	5
atsz–38a	Atlantic Source Zone	-58.6079	13.8503	170.2	15	17.94
atsz–38b	Atlantic Source Zone	-58.1674	13.9240	170.2	15	5
atsz–39a	Atlantic Source Zone	-58.6667	14.3915	146.8	15	17.94
atsz–39b	Atlantic Source Zone	-58.2913	14.6287	146.8	15	5
atsz–39y	Atlantic Source Zone	-59.4168	13.9171	146.8	15	43.82
atsz–39z	Atlantic Source Zone	-59.0415	14.1543	146.8	15	30.88
atsz–40a	Atlantic Source Zone	-59.1899	15.2143	156.2	15	17.94
atsz–40b	Atlantic Source Zone	-58.7781	15.3892	156.2	15	5
atsz–40y	Atlantic Source Zone	-60.0131	14.8646	156.2	15	43.82
atsz–40z	Atlantic Source Zone	-59.6012	15.0395	156.2	15	30.88
atsz–41a	Atlantic Source Zone	-59.4723	15.7987	146.3	15	17.94
atsz–41b	Atlantic Source Zone	-59.0966	16.0392	146.3	15	5
atsz–41y	Atlantic Source Zone	-60.2229	15.3177	146.3	15	43.82
atsz–41z	Atlantic Source Zone	-59.8473	15.5582	146.3	15	30.88
atsz–42a	Atlantic Source Zone	-59.9029	16.4535	137	15	17.94
atsz–42b	Atlantic Source Zone	-59.5716	16.7494	137	15	5
atsz–42y	Atlantic Source Zone	-60.5645	15.8616	137	15	43.82
atsz–42z	Atlantic Source Zone	-60.2334	16.1575	137	15	30.88
atsz–43a	Atlantic Source Zone	-60.5996	17.0903	138.7	15	17.94
atsz–43b	Atlantic Source Zone	-60.2580	17.3766	138.7	15	5
atsz–43y	Atlantic Source Zone	-61.2818	16.5177	138.7	15	43.82
atsz–43z	Atlantic Source Zone	-60.9404	16.8040	138.7	15	30.88
atsz–44a	Atlantic Source Zone	-61.1559	17.8560	141.1	15	17.94
atsz–44b	Atlantic Source Zone	-60.8008	18.1286	141.1	15	5
atsz–44y	Atlantic Source Zone	-61.8651	17.3108	141.1	15	43.82
atsz–44z	Atlantic Source Zone	-61.5102	17.5834	141.1	15	30.88
atsz–45a	Atlantic Source Zone	-61.5491	18.0566	112.8	15	17.94
atsz–45b	Atlantic Source Zone	-61.3716	18.4564	112.8	15	5
atsz–45y	Atlantic Source Zone	-61.9037	17.2569	112.8	15	43.82
atsz–45z	Atlantic Source Zone	-61.7260	17.6567	112.8	15	30.88
atsz–46a	Atlantic Source Zone	-62.4217	18.4149	117.9	15	17.94
atsz–46b	Atlantic Source Zone	-62.2075	18.7985	117.9	15	5
atsz–46y	Atlantic Source Zone	-62.8493	17.6477	117.9	15	43.82
atsz–46z	Atlantic Source Zone	-62.6352	18.0313	117.9	15	30.88

Segment	Description	Longitude(°E)	Latitude(°N)	Strike(°)	Dip(°)	Depth (km)
atsz–47a	Atlantic Source Zone	-63.1649	18.7844	110.5	20	22.1
atsz–47b	Atlantic Source Zone	-63.0087	19.1798	110.5	20	5
atsz–47y	Atlantic Source Zone	-63.4770	17.9936	110.5	20	56.3
atsz–47z	Atlantic Source Zone	-63.3205	18.3890	110.5	20	39.2
atsz–48a	Atlantic Source Zone	-63.8800	18.8870	95.37	20	22.1
atsz–48b	Atlantic Source Zone	-63.8382	19.3072	95.37	20	5
atsz–48y	Atlantic Source Zone	-63.9643	18.0465	95.37	20	56.3
atsz–48z	Atlantic Source Zone	-63.9216	18.4667	95.37	20	39.2
atsz–49a	Atlantic Source Zone	-64.8153	18.9650	94.34	20	22.1
atsz–49b	Atlantic Source Zone	-64.7814	19.3859	94.34	20	5
atsz–49y	Atlantic Source Zone	-64.8840	18.1233	94.34	20	56.3
atsz–49z	Atlantic Source Zone	-64.8492	18.5442	94.34	20	39.2
atsz–50a	Atlantic Source Zone	-65.6921	18.9848	89.59	20	22.1
atsz–50b	Atlantic Source Zone	-65.6953	19.4069	89.59	20	5
atsz–50y	Atlantic Source Zone	-65.6874	18.1407	89.59	20	56.3
atsz–50z	Atlantic Source Zone	-65.6887	18.5628	89.59	20	39.2
atsz–51a	Atlantic Source Zone	-66.5742	18.9484	84.98	20	22.1
atsz–51b	Atlantic Source Zone	-66.6133	19.3688	84.98	20	5
atsz–51y	Atlantic Source Zone	-66.4977	18.1076	84.98	20	56.3
atsz–51z	Atlantic Source Zone	-66.5353	18.5280	84.98	20	39.2
atsz–52a	Atlantic Source Zone	-67.5412	18.8738	85.87	20	22.1
atsz–52b	Atlantic Source Zone	-67.5734	19.2948	85.87	20	5
atsz–52y	Atlantic Source Zone	-67.4781	18.0319	85.87	20	56.3
atsz–52z	Atlantic Source Zone	-67.5090	18.4529	85.87	20	39.2
atsz–53a	Atlantic Source Zone	-68.4547	18.7853	83.64	20	22.1
atsz–53b	Atlantic Source Zone	-68.5042	19.2048	83.64	20	5
atsz–53y	Atlantic Source Zone	-68.3575	17.9463	83.64	20	56.3
atsz–53z	Atlantic Source Zone	-68.4055	18.3658	83.64	20	39.2
atsz–54a	Atlantic Source Zone	-69.6740	18.8841	101.5	20	22.1
atsz–54b	Atlantic Source Zone	-69.5846	19.2976	101.5	20	5
atsz–55a	Atlantic Source Zone	-70.7045	19.1376	108.2	20	22.1
atsz–55b	Atlantic Source Zone	-70.5647	19.5386	108.2	20	5
atsz–56a	Atlantic Source Zone	-71.5368	19.3853	102.6	20	22.1
atsz–56b	Atlantic Source Zone	-71.4386	19.7971	102.6	20	5
atsz–57a	Atlantic Source Zone	-72.3535	19.4838	94.2	20	22.1
atsz–57b	Atlantic Source Zone	-72.3206	19.9047	94.2	20	5
atsz–58a	Atlantic Source Zone	-73.1580	19.4498	84.34	20	22.1
atsz–58b	Atlantic Source Zone	-73.2022	19.8698	84.34	20	5
atsz–59a	Atlantic Source Zone	-74.3567	20.9620	259.7	20	22.1
atsz–59b	Atlantic Source Zone	-74.2764	20.5467	259.7	20	5
atsz–60a	Atlantic Source Zone	-75.2386	20.8622	264.2	15	17.94
atsz–60b	Atlantic Source Zone	-75.1917	20.4306	264.2	15	5
atsz–61a	Atlantic Source Zone	-76.2383	20.7425	260.7	15	17.94
atsz–61b	Atlantic Source Zone	-76.1635	20.3144	260.7	15	5
atsz–62a	Atlantic Source Zone	-77.2021	20.5910	259.9	15	17.94
atsz–62b	Atlantic Source Zone	-77.1214	20.1638	259.9	15	5
atsz–63a	Atlantic Source Zone	-78.1540	20.4189	259	15	17.94
atsz–63b	Atlantic Source Zone	-78.0661	19.9930	259	15	5
atsz–64a	Atlantic Source Zone	-79.0959	20.2498	259.2	15	17.94
atsz–64b	Atlantic Source Zone	-79.0098	19.8236	259.2	15	5
atsz–65a	Atlantic Source Zone	-80.0393	20.0773	258.9	15	17.94
atsz–65b	Atlantic Source Zone	-79.9502	19.6516	258.9	15	5
atsz–66a	Atlantic Source Zone	-80.9675	19.8993	258.6	15	17.94
atsz–66b	Atlantic Source Zone	-80.8766	19.4740	258.6	15	5
atsz–67a	Atlantic Source Zone	-81.9065	19.7214	258.5	15	17.94

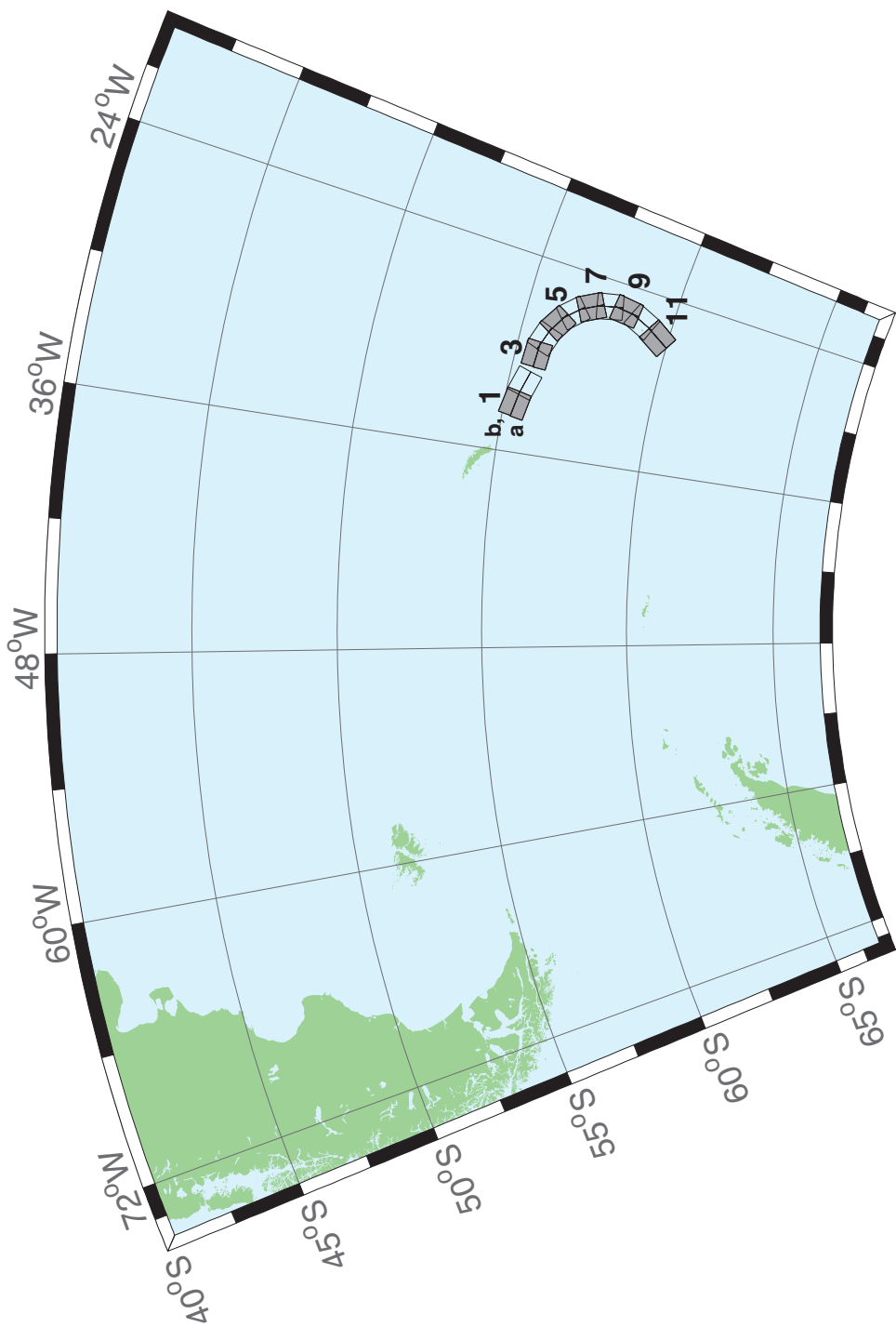| Segment	Description	Longitude(°E)	Latitude(°N)	Strike(°)	Dip(°)	Depth (km)
atsz–67b	Atlantic Source Zone	-81.8149	19.2962	258.5	15	5
atsz–68a	Atlantic Source Zone	-87.8003	15.2509	62.69	15	17.94
atsz–68b	Atlantic Source Zone	-88.0070	15.6364	62.69	15	5
atsz–69a	Atlantic Source Zone	-87.0824	15.5331	72.73	15	17.94
atsz–69b	Atlantic Source Zone	-87.2163	15.9474	72.73	15	5
atsz–70a	Atlantic Source Zone	-86.1622	15.8274	70.64	15	17.94
atsz–70b	Atlantic Source Zone	-86.3120	16.2367	70.64	15	5
atsz–71a	Atlantic Source Zone	-85.3117	16.1052	73.7	15	17.94
atsz–71b	Atlantic Source Zone	-85.4387	16.5216	73.7	15	5
atsz–72a	Atlantic Source Zone	-84.3470	16.3820	69.66	15	17.94
atsz–72b	Atlantic Source Zone	-84.5045	16.7888	69.66	15	5
atsz–73a	Atlantic Source Zone	-83.5657	16.6196	77.36	15	17.94
atsz–73b	Atlantic Source Zone	-83.6650	17.0429	77.36	15	5
atsz–74a	Atlantic Source Zone	-82.7104	16.7695	82.35	15	17.94
atsz–74b	Atlantic Source Zone	-82.7709	17.1995	82.35	15	5
atsz–75a	Atlantic Source Zone	-81.7297	16.9003	79.86	15	17.94
atsz–75b	Atlantic Source Zone	-81.8097	17.3274	79.86	15	5
atsz–76a	Atlantic Source Zone	-80.9196	16.9495	82.95	15	17.94
atsz–76b	Atlantic Source Zone	-80.9754	17.3801	82.95	15	5
atsz–77a	Atlantic Source Zone	-79.8086	17.2357	67.95	15	17.94
atsz–77b	Atlantic Source Zone	-79.9795	17.6378	67.95	15	5
atsz–78a	Atlantic Source Zone	-79.0245	17.5415	73.61	15	17.94
atsz–78b	Atlantic Source Zone	-79.1532	17.9577	73.61	15	5
atsz–79a	Atlantic Source Zone	-78.4122	17.5689	94.07	15	17.94
atsz–79b	Atlantic Source Zone	-78.3798	18.0017	94.07	15	5
atsz–80a	Atlantic Source Zone	-77.6403	17.4391	103.3	15	17.94
atsz–80b	Atlantic Source Zone	-77.5352	17.8613	103.3	15	5
atsz–81a	Atlantic Source Zone	-76.6376	17.2984	98.21	15	17.94
atsz–81b	Atlantic Source Zone	-76.5726	17.7278	98.21	15	5
atsz–82a	Atlantic Source Zone	-75.7299	19.0217	260.1	15	17.94
atsz–82b	Atlantic Source Zone	-75.6516	18.5942	260.1	15	5
atsz–83a	Atlantic Source Zone	-74.8351	19.2911	260.8	15	17.94
atsz–83b	Atlantic Source Zone	-74.7621	18.8628	260.8	15	5
atsz–84a	Atlantic Source Zone	-73.6639	19.2991	274.8	15	17.94
atsz–84b	Atlantic Source Zone	-73.7026	18.8668	274.8	15	5
atsz–85a	Atlantic Source Zone	-72.8198	19.2019	270.6	15	17.94
atsz–85b	Atlantic Source Zone	-72.8246	18.7681	270.6	15	5
atsz–86a	Atlantic Source Zone	-71.9143	19.1477	269.1	15	17.94
atsz–86b	Atlantic Source Zone	-71.9068	18.7139	269.1	15	5
atsz–87a	Atlantic Source Zone	-70.4738	18.8821	304.5	15	17.94
atsz–87b	Atlantic Source Zone	-70.7329	18.5245	304.5	15	5
atsz–88a	Atlantic Source Zone	-69.7710	18.3902	308.9	15	17.94
atsz–88b	Atlantic Source Zone	-70.0547	18.0504	308.4	15	5
atsz–89a	Atlantic Source Zone	-69.2635	18.2099	283.9	15	17.94
atsz–89b	Atlantic Source Zone	-69.3728	17.7887	283.9	15	5
atsz–90a	Atlantic Source Zone	-68.5059	18.1443	272.9	15	17.94
atsz–90b	Atlantic Source Zone	-68.5284	17.7110	272.9	15	5
atsz–91a	Atlantic Source Zone	-67.6428	18.1438	267.8	15	17.94
atsz–91b	Atlantic Source Zone	-67.6256	17.7103	267.8	15	5
atsz–92a	Atlantic Source Zone	-66.8261	18.2536	262	15	17.94
atsz–92b	Atlantic Source Zone	-66.7627	17.8240	262	15	5

Figure B.2: South Sandwich Islands Subduction Zone.

Table B.2: Earthquake parameters for South Sandwich Islands Subduction Zone unit sources.

Segment	Description	Longitude(°E)	Latitude(°N)	Strike(°)	Dip(°)	Depth (km)
sssz–1a	South Sandwich Islands Subduction Zone	-33.0670	-55.3780	280.2	15	17.94
sssz–1b	South Sandwich Islands Subduction Zone	-32.9242	-54.9510	280.2	15	5
sssz–2a	South Sandwich Islands Subduction Zone	-31.7197	-55.5621	286.3	15	17.94
sssz–2b	South Sandwich Islands Subduction Zone	-31.4969	-55.1457	286.3	15	5
sssz–3a	South Sandwich Islands Subduction Zone	-29.8355	-55.7456	273	15	17.94
sssz–3b	South Sandwich Islands Subduction Zone	-29.7873	-55.3123	273	15	5
sssz–4a	South Sandwich Islands Subduction Zone	-28.7648	-55.8715	290	15	17.94
sssz–4b	South Sandwich Islands Subduction Zone	-28.4930	-55.4638	290	15	5
sssz–5a	South Sandwich Islands Subduction Zone	-27.6356	-56.1844	301.5	15	17.94
sssz–5b	South Sandwich Islands Subduction Zone	-27.2218	-55.8143	301.5	15	5
sssz–6a	South Sandwich Islands Subduction Zone	-26.7655	-56.5959	317.5	15	17.94
sssz–6b	South Sandwich Islands Subduction Zone	-26.1774	-56.3029	317.5	15	5
sssz–7a	South Sandwich Islands Subduction Zone	-26.0921	-57.1441	332.1	15	17.94
sssz–7b	South Sandwich Islands Subduction Zone	-25.3776	-56.9411	332.1	15	5
sssz–8a	South Sandwich Islands Subduction Zone	-25.7129	-57.7563	347.9	15	17.94
sssz–8b	South Sandwich Islands Subduction Zone	-24.9088	-57.6652	347.9	15	5
sssz–9a	South Sandwich Islands Subduction Zone	-25.7003	-58.3505	7.182	15	17.94
sssz–9b	South Sandwich Islands Subduction Zone	-24.8687	-58.4047	7.182	15	5
sssz–10a	South Sandwich Islands Subduction Zone	-26.0673	-58.9577	24.25	15	17.94
sssz–10b	South Sandwich Islands Subduction Zone	-25.2869	-59.1359	24.25	15	5
sssz–11a	South Sandwich Islands Subduction Zone	-26.8279	-59.6329	32.7	15	17.94
sssz–11b	South Sandwich Islands Subduction Zone	-26.0913	-59.8673	32.7	15	5

Authors: Lindsey Wright

1.0 PURPOSE

Forecast models are tested with synthetic tsunami events covering a range of tsunami source locations and magnitudes. Testing is also done with selected historical tsunami events when available.

The purpose of forecast model testing is three-fold. The first objective is to assure that the results obtained with the NOAA's tsunami forecast system software, which has been released to the Tsunami Warning Centers for operational use, are consistent with those obtained by the researcher during the development of the forecast model. The second objective is to test the forecast model for consistency, accuracy, time efficiency, and quality of results over a range of possible tsunami locations and magnitudes. The third objective is to identify bugs and issues in need of resolution by the researcher who developed the Forecast Model or by the forecast system software development team before the next version release to NOAA's two Tsunami Warning Centers.

Local hardware and software applications, and tools familiar to the researcher(s), are used to run the Method of Splitting Tsunamis (MOST) model during the forecast model development. The test results presented in this report lend confidence that the model performs as developed and produces the same results when initiated within the forecast system application in an operational setting as those produced by the researcher during the forecast model development. The test results assure those who rely on the Savannah tsunami forecast model that consistent results are produced irrespective of system.

2.0 TESTING PROCEDURE

The general procedure for forecast model testing is to run a set of synthetic tsunami scenarios and a selected set of historical tsunami events through the forecast system application and compare the results with those obtained by the researcher during the forecast model development and presented in the Tsunami Forecast Model Report. Specific steps taken to test the model include:

1. Identification of testing scenarios, including the standard set of synthetic events, appropriate historical events, and customized synthetic scenarios that may have been used by the researcher(s) in developing the forecast model.
2. Creation of new events to represent customized synthetic scenarios used by the researcher(s) in developing the forecast model, if any.
3. Submission of test model runs with the forecast system, and export of the results from A, B, and C grids, along with time series.
4. Recording applicable metadata, including the specific forecast system version used for testing.
5. Examination of forecast model results for instabilities in both time series and plot results.
6. Comparison of forecast model results obtained through the forecast system with those obtained during the forecast model development.
7. Summarization of results with specific mention of quality, consistency, and time efficiency.
8. Reporting of issues identified to modeler and forecast system software development team.
9. Retesting the forecast models in the forecast system when reported issues have been addressed or explained.

Synthetic model runs were tested on a DELL PowerEdge R510 computer equipped with two Xeon E5670 processors at 2.93 Ghz, each with 12 MBytes of cache and 32GB memory. The processors are hex core and support hyperthreading, resulting in the computer performing as a 24 processor core machine. Additionally, the testing computer supports 10 Gigabit Ethernet for fast network connections. This computer configuration is similar or the same as the configurations of the computers installed at the Tsunami Warning Centers so the compute times should only vary slightly.

Results

The Ponce forecast model was tested with SIFT version 3.2.

The Ponce, Puerto Rico forecast model was tested with three synthetic scenarios. Test results from the forecast system and comparisons with the results obtained during the forecast model development are shown numerically in Table 1 and graphically in Figures 1 to 3. The results show that the minimum and maximum amplitudes and time series obtained from the forecast system agree with those obtained during the forecast model development, and that the forecast model is stable and robust, with consistent and high quality results across geographically distributed tsunami sources. The model run time (wall clock time) was less than 36.5 minutes for 12 hours of simulation time, and 12 minutes for 4.0 hours. This run time is not within the 10 minute run time for 4 hours of simulation time.

A suite of three synthetic events was run on the Ponce forecast model. The modeled scenarios were stable for all cases run with no inconsistencies or ringing. The largest modeled height was 342 centimeters (cm) from the Atlantic (ATSZ 48-57) source zone. The smallest signal of 19 cm was recorded at the far field South Sandwich (SSSZ 1-10) source zone. Maximum and minimum values and visual comparisons between the development cases and the forecast system output were consistent in shape and amplitude for all cases run. The Ponce reference point used for the forecast model development is the same as what is deployed in the forecast system, so the results can be considered valid for the three cases studied.
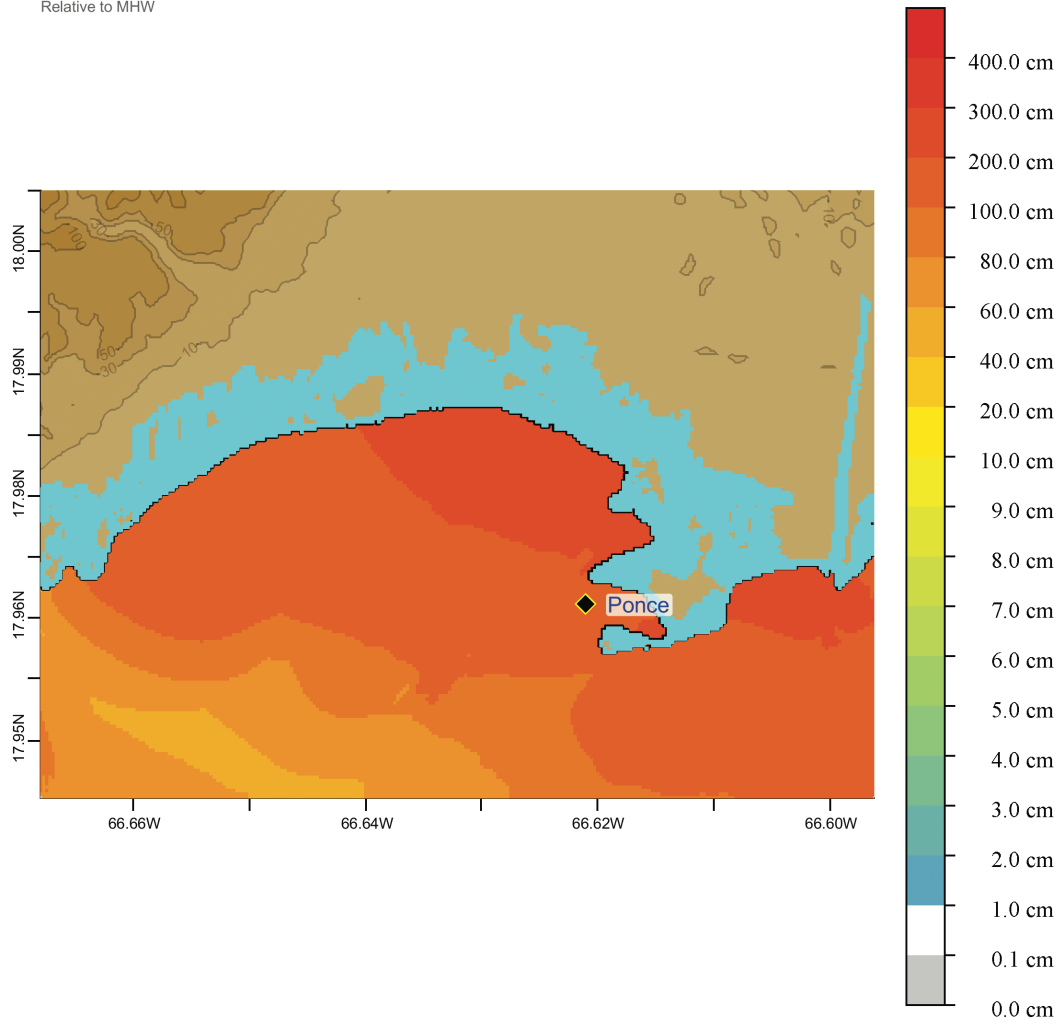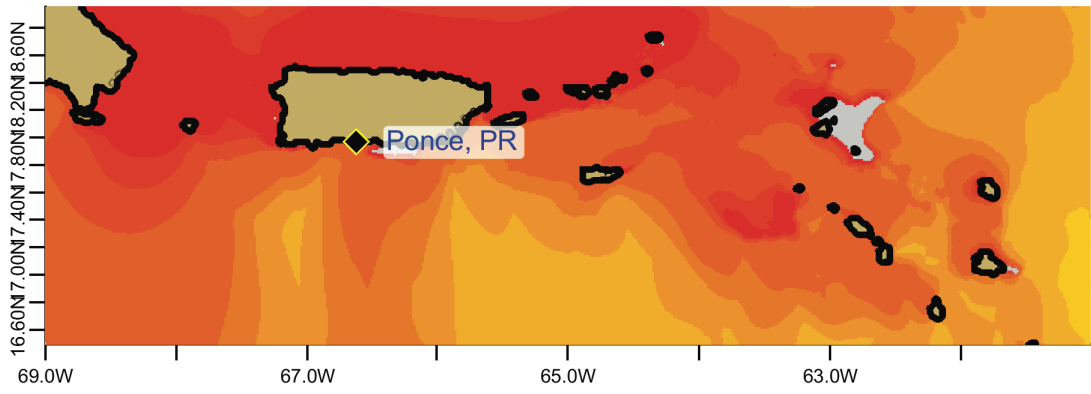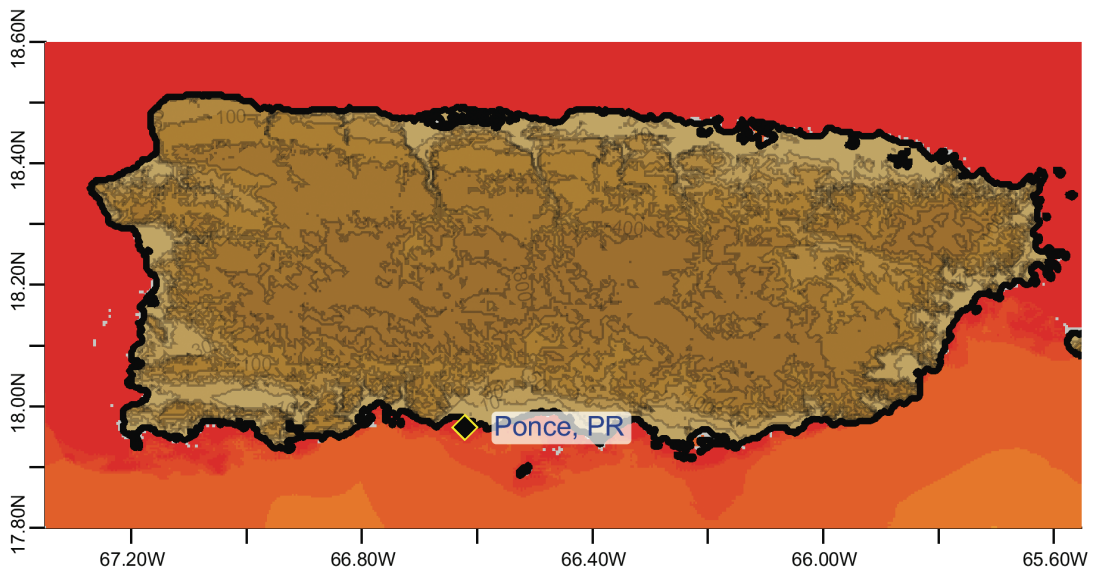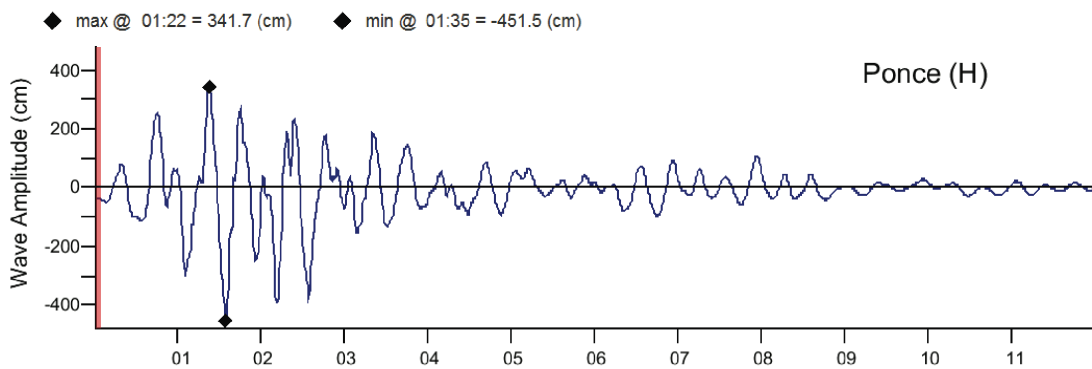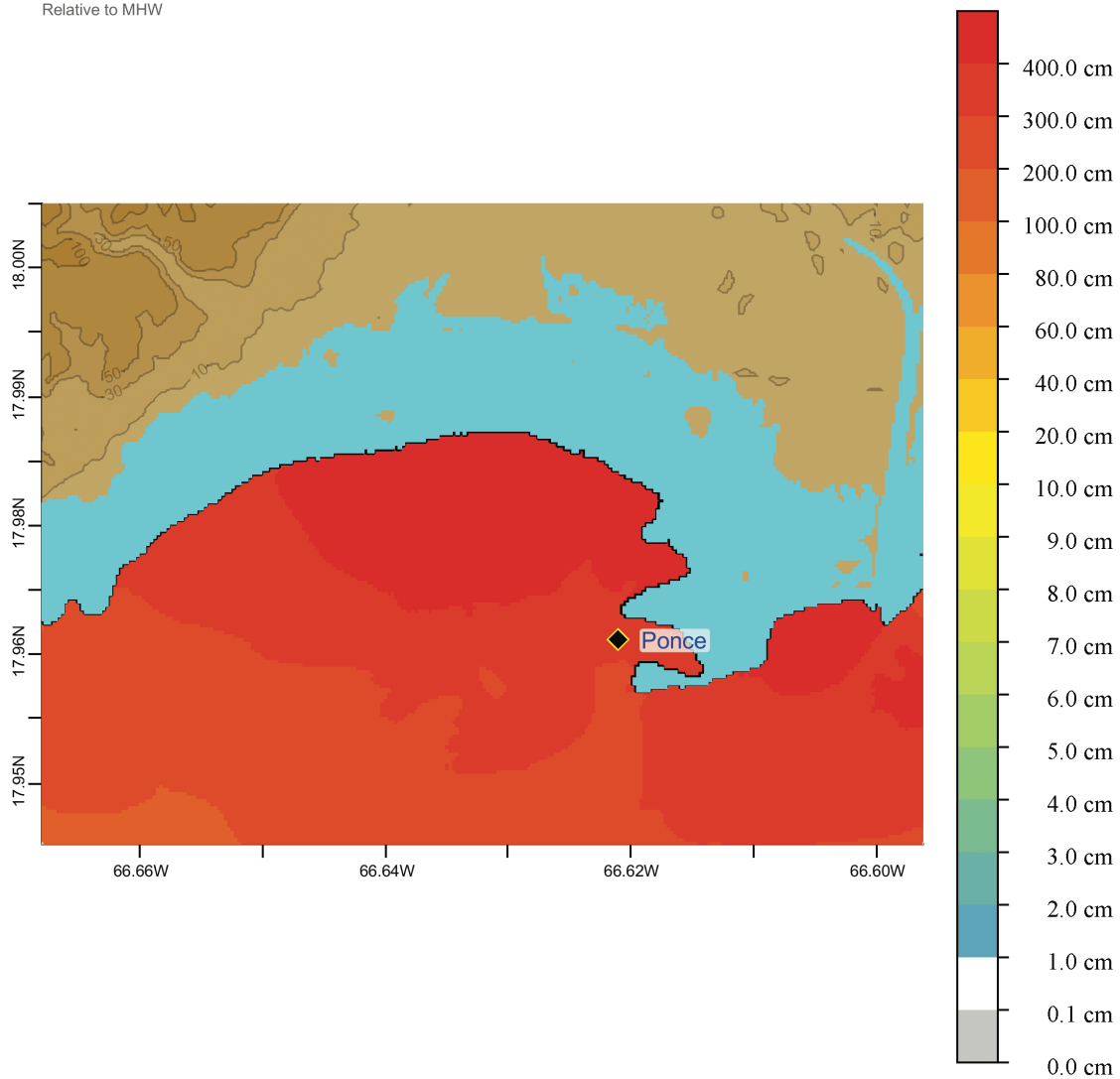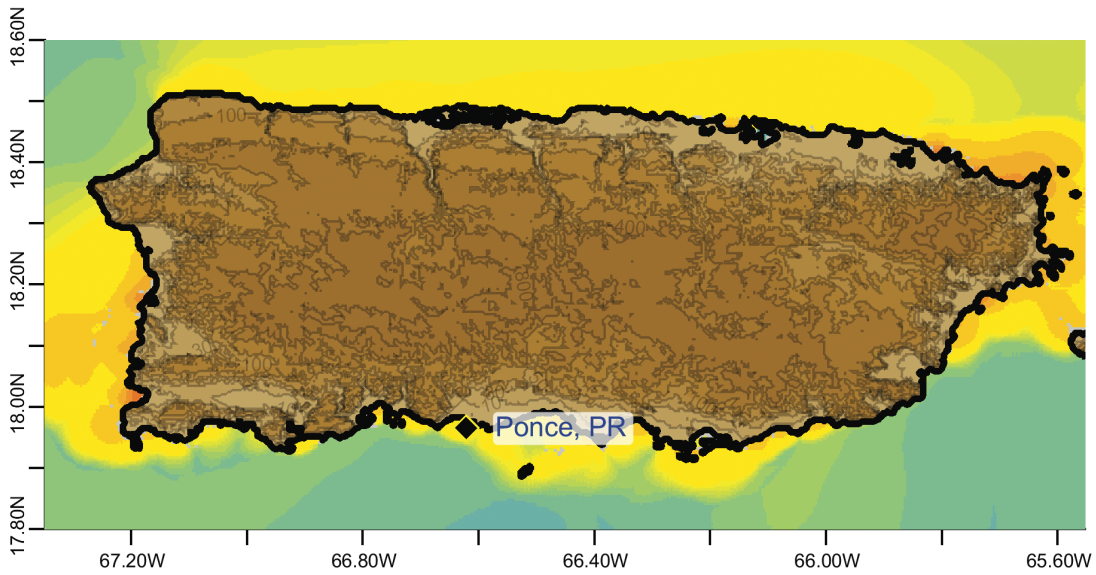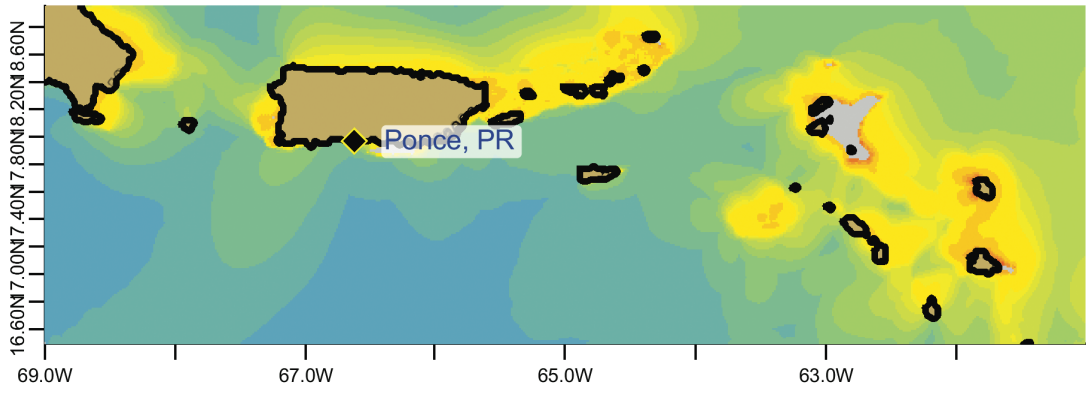
List of Figures
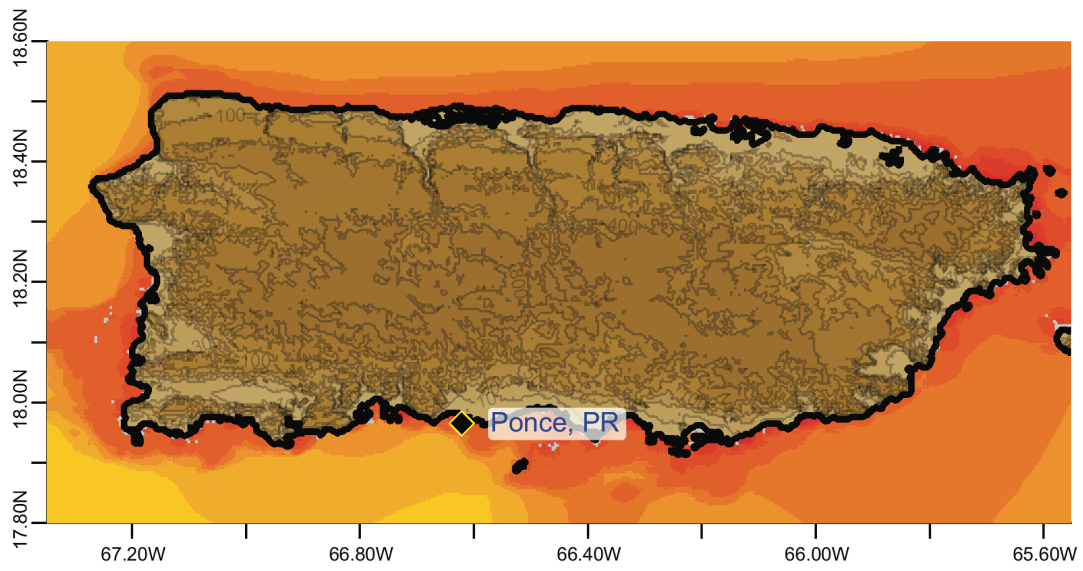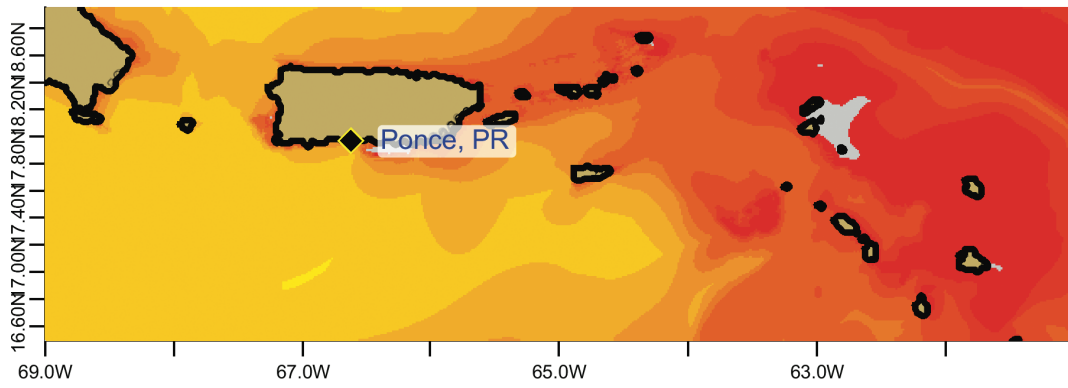
Ponce, PR

Ponce, PR
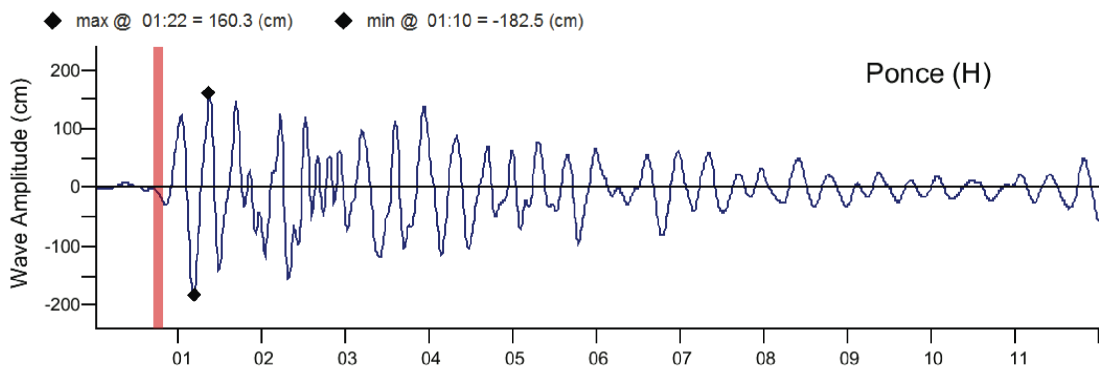
Figure 1: Response of the Ponce forecast model to synthetic scenario ATSZ 38-47 (alpha=25). Maximum sea surface elevation for (a) A-grid, b) B-grid, c) C-grid. Sea surface elevation time series at the C-grid warning point (d) The lower time series plot is the result obtained during model development and is shown for comparison with test results.

Figure 2: Response of the Ponce forecast model to synthetic scenario ATSZ 48-57 (alpha=25). Maximum sea surface elevation for (a) A-grid, b) B-grid, c) C-grid. Sea surface elevation time series at the C-grid warning point (d) The lower time series

plot is the result obtained during model development and is shown for comparison with test results.
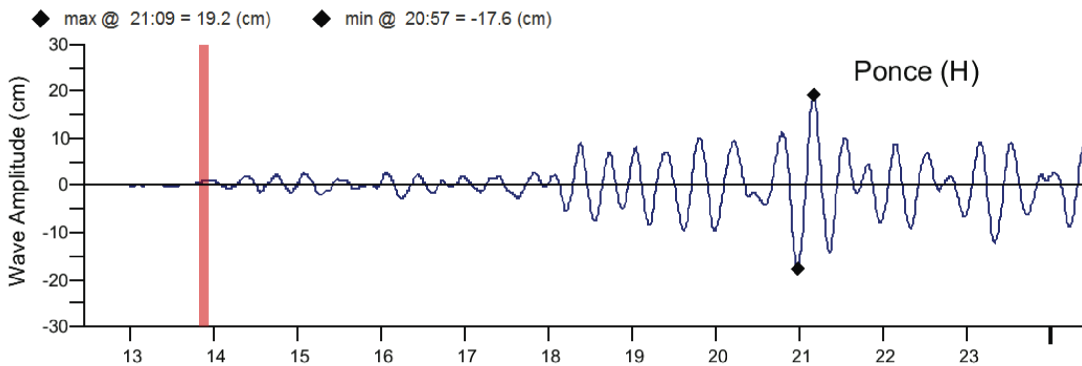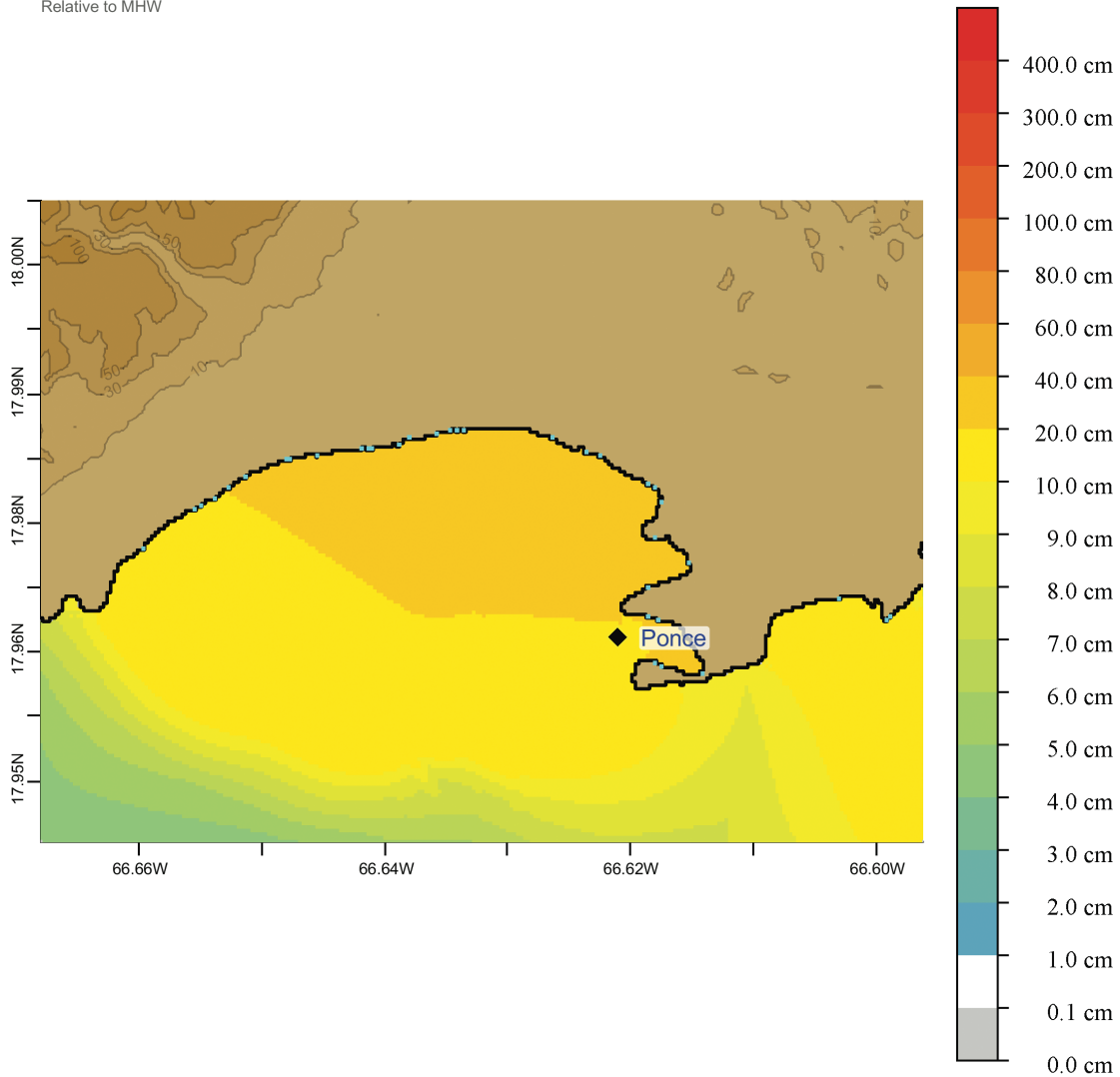
Figure 3: Response of the Ponce forecast model to synthetic scenario SSSZ 1-10 (alpha=25). Maximum sea surface elevation for (a) A-grid, b) B-grid, c) C-grid. Sea surface elevation time series at the C-grid warning point (d) The lower time series

plot is the result obtained during model development and is shown for comparison with test results.

List of Tables

Scenario Name	Source Zone	Tsunami Source	α [m]	SIFT Max (cm)	Developr t Max (c
		Mega-tsunami Scenarios			
ATSZ 38-47	Atlantic	A38-A47, B38-B47	25	160.3	160.23
ATSZ 48-57	Atlantic	A48-A57, B48-B57	25	341.7	341.5
SSSZ 1-10	South Sandwich	A1-A10, B1-B10	25	19.2	19.2

Table 1. Table of maximum and minimum amplitudes at Ponce, Puerto Rico
warning point for synthetic and historical events tested using SIFT.